




# Novel *N*-(Substituted) Thioacetamide Quinazolinone Benzenesulfonamides as Antimicrobial Agents

This article was published in the following Dove Press journal:  
International Journal of Nanomedicine

Mostafa M Ghorab<sup>1</sup>   
Ali S Alqahtani<sup>2,3</sup>  
Aiten M Soliman<sup>1</sup>   
Ahmed A Askar<sup>4</sup> 

<sup>1</sup>Department of Drug Radiation Research, National Center for Radiation Research and Technology (NCRRT), Egyptian Atomic Energy Authority (EAEA), Cairo 11765, Egypt; <sup>2</sup>Medicinal, Aromatic and Poisonous Plants Research Center (MAPPRC), College of Pharmacy, King Saud University, Riyadh 11451, Saudi Arabia; <sup>3</sup>Department of Pharmacognosy, College of Pharmacy, King Saud University, Riyadh 11451, Saudi Arabia; <sup>4</sup>Botany and Microbiology Department, Faculty of Science (Boys), Al-Azhar University, Cairo, Egypt

**Aim:** With the rapid emergence of antibiotic resistance, efforts are being made to obtain new selective antimicrobial agents. Hybridization between quinazolinone and benzenesulfonamide can provide new antimicrobial candidates. Also, the use of nanoparticles can help boost drug efficacy and lower side effects.

**Materials and Methods:** Novel quinazolinone-benzenesulfonamide derivatives **5–18** were synthesized and screened for their antimicrobial activity against Gram-positive bacteria, Gram-negative bacteria, MRSA and yeast. The most potent compound **16** was conjugated with copper oxide nanoparticles 16-CuONPs by gamma irradiation (4.5 KGy). Characterization was performed using UV-Visible, TEM examination, XRD patterns and DLS. Moreover, compound **16** was used to synthesize two nanoformulations: 16-CNPs by loading **16** in chitosan nanoparticles and the nanocomposites 16-CuONPs-CNPs. Characterization of these nanoformulations was performed using TEM and zeta potential. Besides, the inhibitory profile against *Staphylococcus aureus* DNA gyrase was assayed. Cytotoxic evaluation of **16**, 16-CNPs and 16-CuONPs-CNPs on normal VERO cell line was carried out to determine its relative safety. Molecular docking of **16** was performed inside the active site of *S. aureus* DNA gyrase. **Results:** Compound **16** was the most active in this series against all the tested strains and showed inhibition zones and MICs in the ranges of 25–36 mm and 0.31–5.0 µg/mL, respectively. The antimicrobial screening of the synthesized nanoformulations revealed that 16-CuONPs-CNPs displayed the most potent activity. The MBCs of **16** and the nanoformulations were measured and proved their bactericidal mode of action. The inhibitory profile against *S. aureus* DNA gyrase showed IC<sub>50</sub> ranging from 10.57 to 27.32 µM. Cytotoxic evaluation of **16**, 16-CNPs and 16-CuONPs-CNPs against normal VERO cell lines proved its relative safety (IC<sub>50</sub>= 927, 543 and 637 µg/mL, respectively). Molecular docking of **16** inside the active site of *S. aureus* DNA gyrase showed that it binds in the same manner as that of the co-crystallized ligand, ciprofloxacin.

**Conclusion:** Compound **16** could be considered as a new antimicrobial lead candidate with enhanced activity upon nanoformulation.

**Keywords:** quinazolinone, benzenesulfonamide, antimicrobial, nanoparticles, nanoformulations, MBC, *Staphylococcus aureus* DNA gyrase, docking

## Introduction

The exploration of new antimicrobial agents is essentially required in order to defeat the rapid emergence of drug resistance and toxicity.<sup>1–4</sup> The misuse and overconsumption of antibiotics (AB) have led to the evolution of resistant strains. An example of major concern is the development of AB-resistance in *S. aureus* (MRSA), which is frequently linked to hospital and community-acquired infections.<sup>5,6</sup>

Correspondence: Mostafa M Ghorab; Ali S Alqahtani  
Tel +20 1067846727  
Email mmsghorab@yahoo.com; Alalqahtani@ksu.edu.sa

Quinazolinone is a privileged structure that possesses activity as anticancer, antiviral, antibacterial, antifungal, anti-tubercular and herbicidal.<sup>7–10</sup> Some quinazolinone derivatives act as chemo-sensitizers of antibiotic activity to *Enterobacter aerogenes*, *Klebsiella pneumoniae*, *Pseudomonas aeruginosa* resistant strains,<sup>11</sup> *Escherichia Coli*, *Staphylococcus aureus*, *Bacillus subtilis* and pathogenic fungi as *Saccharomyces cerevisiae* and *Candida albicans*.<sup>12</sup> Other alkylamino quinazolinone derivatives were reported to restore AB-activity in Gram-negative isolates.<sup>13</sup> Devi et al reported a series of new aza isatin derivatives containing quinazolinones (A) as potent antimicrobial agents.<sup>14,15</sup> Suresha and his coworkers revealed a series of urea, thiourea, acetamide and sulfonamide derivatives of quinazolinone (B and C) as potent antibacterial agents.<sup>16</sup> Al-Omary et al described some new 2-alkyl thioquinazolinones to act as nonclassical antifolates (D).<sup>17</sup> Also, Dinakaran et al proved that the substitution at position 3 of quinazolin-4(3H)-ones is associated with antimicrobial properties (Figure 1).<sup>18</sup> On the other hand, sulfonamides retain its antimicrobial activity by manifesting the antagonistic properties of *p*-aminobenzoic acid and blocking the SH, NH<sub>2</sub>-containing enzymes and proteins.<sup>19,20</sup>

The use of nanoparticles (NPs) has been widely spread in the pharmaceutical field due to the following advantages; the size and surface of the drug can be easily manipulated, it is feasible to sustain the drug release in the gastrointestinal tract, and to boost drug efficacy with lowering the side effects by controlling the clearance of the drug from the body.<sup>21</sup> Chitosan (CS), a natural polysaccharide, is the most frequently used polymer in drug delivery systems, due to its biological, biodegradable and antibacterial properties.<sup>22</sup> The antibacterial activity of some drugs can be effectively enhanced by its incorporation into chitosan NPs (CNP). CNPs are active against *E. coli* and *B. subtilis*.<sup>23</sup> It is indicated that its antibacterial activity is due to the penetration of the cell membrane causing the effusion of the cytoplasm and cell death.<sup>24</sup> The presence of chelating sites (NH<sub>2</sub> and OH) in chitosan structure aids in chemical reactions as metal ion sorption through electrostatic attraction and ion exchange for metal anions in acidic solutions forming the nanocomposites, which are promising NPs for reducing the bacteria-associated infections.<sup>25,26</sup> Furthermore, the metal NPs exert the antibacterial effect by their small size and high surface to volume ratio, which allow them to closely adhere to the microbial membranes.<sup>27,28</sup> An example of such metal NPs is copper oxide NPs (CuONPs), characterized by their low toxicity, heat resistance and broad-spectrum activity against

Gram-positive bacteria, Gram-negative bacteria, MRSA and *Candida albicans*.<sup>25,29</sup>

Hybridization has proven to be beneficial for the preparation of new antimicrobial agents and overcoming the drawbacks of the conventionally used drugs.<sup>4,30</sup> So, sulfonamides were integrated with quinazolin-4(3H)-ones in order to obtain more potent candidates. As a continuation of our previous efforts,<sup>12,31–35</sup> we synthesized new quinazolinone derivatives bearing benzenesulfonamide in order to study their antimicrobial activity. The synthesized compounds were tested against Gram-positive bacteria, Gram-negative bacteria, MRSA and *Candida*. The most potent compound was conjugated to copper oxide nanoparticles (CuONPs) (by the aid of gamma irradiation) and incorporated into two nanoformulations; chitosan nanoparticles (CNP) and copper oxide nanoparticles incorporated into chitosan, in order to detect the variation in antimicrobial activity. Also, an in-vitro enzyme assay was performed for the most potent compound and the nanoformulations against *S. aureus* DNA gyrase. DNA gyrase is considered a fundamental type II DNA topoisomerase that maneuvers DNA topology by making temporary double-strand breaks and DNA strand passage.<sup>36</sup> It is considered as an important drug target due to its vital role in bacterial survival.<sup>37</sup> An example of DNA gyrase poisons of commercial importance is ciprofloxacin (Figure 1). Furthermore, the cytotoxicity of the most potent compound and the nanoformulations were evaluated against VERO (African green monkey kidney epithelial cells) normal cell line. Molecular docking was used to confirm the possible binding interactions of this compound into the active site of *S. aureus* DNA gyrase to assert the biological activity results.

## Materials and Methods

### Chemistry

Uncorrected Melting points were determined on a Gallen Kamp apparatus (Sanyo Gallen Kamp, UK). Thin-layer chromatography (TLC) was performed on precoated silica gel plates (*Kieselgel* 0.25 mm, 60 F254, Merck, Germany) with a solvent system of chloroform/methanol (8:2). The IR spectra used to determine the functional group within the molecule were recorded using an FT-IR spectrophotometer (Perkin Elmer, USA). NMR spectra used for structural determination of molecules using the <sup>1</sup>H and <sup>13</sup>C atoms were scanned on an NMR spectrophotometer (Bruker AXS Inc., Switzerland), operating at 500 MHz for <sup>1</sup>H and 125.76 MHz for <sup>13</sup>C. Chemical

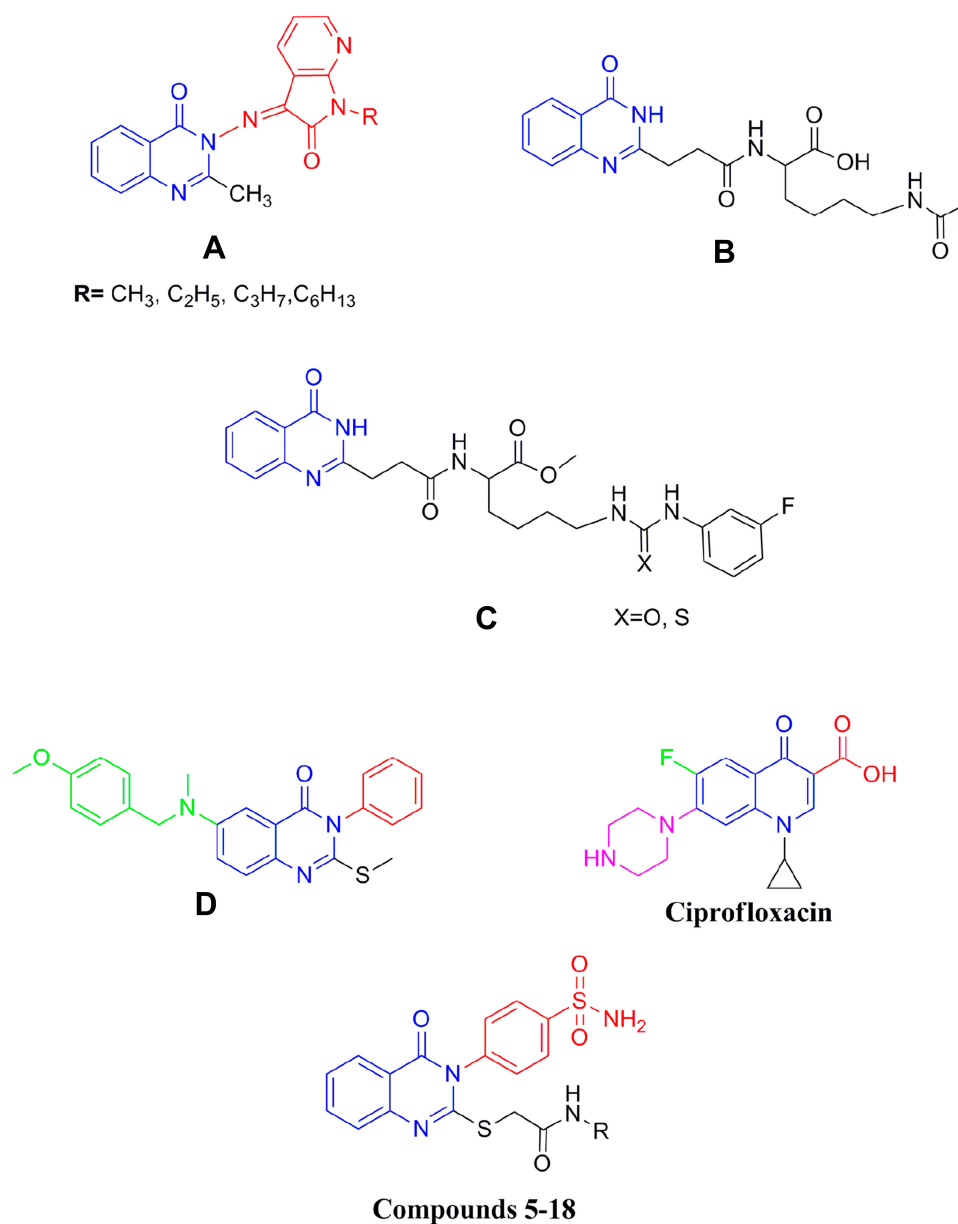


**Figure 1** Quinazolinone-based antimicrobial agents and ciprofloxacin.

shifts were expressed in  $\delta$ -values (ppm) relative to TMS, using DMSO- $d_6$  as a solvent. Mass spectra showing fragmentation patterns were characterized by their mass to charge ratios ( $m/z$ ) and relative abundances and were recorded on an ISQ LT Thermo Scientific GCMS model (Massachusetts, USA). Elemental analyses were used to determine the quantity of a particular element within the molecule and were performed on a model 2400 CHNSO analyzer (Perkin Elmer, USA). All the values were within  $\pm 0.4\%$  of the theoretical values.

#### 4-(2-Mercapto-4-oxoquinazolin-3(4H)-yl) Benzenesulfonamide (**4**)<sup>38</sup>

##### General Procedure for the Synthesis of 2-((4-Oxo-3-(4-sulfamoylphenyl)-3,4-dihydroquinazolin-2-yl)thio)-N-substituted acetamide **5-18**

A mixture of **4** (3.33 g, 0.01 mol) and 2-chloro-N-substituted acetamide (0.01 mol) in dry acetone (30 mL) and anhydrous K<sub>2</sub>CO<sub>3</sub> (1.38 g, 0.01 mol) was stirred at room temperature for 12 hrs, filtered and the solid obtained was crystallized from ethanol to give **5-18**.

**2-((4-Oxo-3-(4-sulfamoylphenyl)-3,4-dihydroquinazolin-2-yl)thio)-N-phenylacetamide (5)**

**5:** Yield, 87%; m.p. 269.0°C. IR: 3447, 3319, 3211 (NH<sub>2</sub>, NH), 3098 (arom.), 2926, 2837 (aliph.), 1701, 1680 (2CO), 1612 (CN), 1334, 1161 (SO<sub>2</sub>). <sup>1</sup>HNMR: 4.13 (s, 2H), 7.06–7.10 (m, 1H), 7.31–7.40 (m, 4H), 7.48 (dd, 1H, *J* = 6 & 2.5 Hz), 7.59–7.69 (m, 2H), 7.71 (d, 2H, *J* = 8 Hz, AB), 7.84 (dd, 1H, *J* = 6 & 2.5 Hz), 8.03 (d, 2H, *J* = 8 Hz, AB), 8.08 (s, 2H), 10.40 (s, 1H). <sup>13</sup>CNMR: 39.47, 119.62 (3), 126.64 (3), 127.36 (2), 129.26 (3), 130.58 (2), 139.40 (3), 147.59 (2), 156.29, 161.17, 166.39. MS *m/z* (%): 466 (M<sup>+</sup>) (19.43), 388 (100). Anal. Calcd. for C<sub>22</sub>H<sub>18</sub>N<sub>4</sub>O<sub>4</sub>S<sub>2</sub> (466.53): C, 56.64; H, 3.89; N, 12.01. Found: C, 56.34; H, 3.57; N, 11.79.

**2-((4-Oxo-3-(4-sulfamoylphenyl)-3,4-dihydroquinazolin-2-yl)thio)-N-2-tolylacetamide (6)**

**6:** Yield, 80%; m.p. 251.5°C. IR: 3410, 3377, 3220 (NH<sub>2</sub>, NH), 3097 (arom.), 2978, 2912 (aliph.), 1701, 1683 (2CO), 1621 (CN), 1399, 1161 (SO<sub>2</sub>). <sup>1</sup>HNMR: 2.20 (s, 3H), 4.16 (s, 2H), 7.08 (ddd, 1H, *J* = 8 & 6 Hz), 7.15 (ddd, 1H, *J* = 8 & 6 Hz), 7.20 (dd, 1H, *J* = 6 & 1.5 Hz), 7.36 (dd, 1H, *J* = 8 & 1.5 Hz), 7.50 (dd, 1H, *J* = 7.5 & 2.5 Hz), 7.63–7.69 (m, 2H), 7.87 (d, 2H, *J* = 7.5 Hz, AB), 8.01 (dd, 1H, *J* = 7.5 & 2.5 Hz), 8.10 (d, 2H, *J* = 7.5 Hz, AB), 8.11 (s, 2H), 9.81 (s, 1H). <sup>13</sup>CNMR: 18.32, 37.07, 125.42 (3), 125.88 (2), 126.43 (2), 127.11, 127.30, 130.50 (2), 132.33 (2), 135.57 (2), 136.56 (2), 147.62, 156.79, 161.10, 166.09. MS *m/z* (%): 480 (M<sup>+</sup>) (24.21), 331 (100). Anal. Calcd. for C<sub>23</sub>H<sub>20</sub>N<sub>4</sub>O<sub>4</sub>S<sub>2</sub> (480.56): C, 57.48; H, 4.19; N, 11.66. Found: C, 57.69; H, 4.44; N, 11.92.

**2-((4-Oxo-3-(4-sulfamoylphenyl)-3,4-dihydroquinazolin-2-yl)thio)-N-3-tolylacetamide (7)**

**7:** Yield, 69%; m.p. 262.4°C. IR: 3427, 3313, 3188 (NH<sub>2</sub>, NH), 3053 (arom.), 2956, 2922 (aliph.), 1681, 1654 (2CO), 1612 (CN), 1332, 1165 (SO<sub>2</sub>). <sup>1</sup>HNMR: 2.24 (s, 3H), 4.11 (s, 2H), 7.10 (ddd, 1H, *J* = 8 & 2 Hz), 7.47 (dd, 1H, *J* = 8 & 6.5 Hz), 7.48–7.61 (m, 5H), 7.76 (d, 2H, *J* = 7 Hz, AB), 7.85 (dd, 1H, *J* = 6 & 1.5 Hz), 8.03 (d, 2H, *J* = 7 Hz, AB), 8.10 (s, 2H), 10.21 (s, 1H). <sup>13</sup>CNMR: 20.90, 37.80, 119.62 (3), 127.47 (3), 129.64 (3), 130.84 (3), 136.05 (2), 138.67 (2), 139.15, 146.82, 158.70, 160.32, 165.72. MS *m/z* (%): 480 (M<sup>+</sup>) (41.81), 373 (100). Anal.

Calcd. for C<sub>23</sub>H<sub>20</sub>N<sub>4</sub>O<sub>4</sub>S<sub>2</sub> (480.56): C, 57.48; H, 4.19; N, 11.66. Found: C, 57.21; H, 4.01; N, 11.35.

**2-((4-Oxo-3-(4-sulfamoylphenyl)-3,4-dihydroquinazolin-2-yl)thio)-N-4-tolylacetamide (8)**

**8:** Yield, 91%; m.p. 315.5°C. IR: 3410, 3376, 3200 (NH<sub>2</sub>, NH), 3076 (arom.), 2966, 2871 (aliph.), 1686, 1661 (2CO), 1611 (CN), 1376, 1156 (SO<sub>2</sub>). <sup>1</sup>HNMR: 2.08 (s, 3H), 4.30 (s, 2H), 7.13–7.34 (m, 4H), 7.47–7.71 (m, 3H), 7.86 (d, 2H, *J* = 6.5 Hz, AB), 7.87 (dd, 1H, *J* = 6 & 2 Hz), 7.94 (d, 2H, *J* = 6.5 Hz, AB), 8.13 (s, 2H), 10.04 (s, 1H). <sup>13</sup>CNMR: 22.13, 31.18, 117.92 (3), 122.38 (3), 126.53 (2), 126.91 (2), 130.44 (3), 134.67 (3), 142.83, 145.05, 150.96, 162.24, 175.02. MS *m/z* (%): 480 (M<sup>+</sup>) (7.12), 91 (100). Anal. Calcd. for C<sub>23</sub>H<sub>20</sub>N<sub>4</sub>O<sub>4</sub>S<sub>2</sub> (480.56): C, 57.48; H, 4.19; N, 11.66. Found: C, 57.73; H, 4.31; N, 12.02.

**N-(2-Ethylphenyl)-2-((4-oxo-3-(4-sulfamoylphenyl)-3,4-dihydroquinazolin-2-yl)thio) acetamide (9)**

**9:** Yield, 68%; m.p. 170.5°C. IR: 3387, 3255, 3186 (NH<sub>2</sub>, NH), 3066 (arom.), 2966, 2927 (aliph.), 1681, 1656 (2CO), 1606 (CN), 1336, 1163 (SO<sub>2</sub>). <sup>1</sup>HNMR: 1.06 (t, 3H, *J* = 10 Hz), 2.58 (q, 2H, *J* = 9.5 Hz), 4.16 (s, 2H), 7.15 (dd, 1H, *J* = 6 & 1.5 Hz), 7.22 (ddd, 1H, *J* = 8 & 6 Hz), 7.32–7.60 (m, 3H), 7.65–7.75 (m, 2H), 7.76 (d, 2H, *J* = 8.5 Hz, AB), 7.88 (dd, 1H, *J* = 6 & 2.5 Hz), 8.04 (d, 2H, *J* = 8.5 Hz, AB), 8.11 (s, 2H), 9.63 (s, 1H). <sup>13</sup>CNMR: 14.64, 24.13, 36.99, 120.52 (3), 126.40 (2), 126.71 (2), 127.10 (2), 127.46, 128.92 (2), 130.84 (3), 139.09 (2), 146.78, 158.60, 161.11, 166.3. MS *m/z* (%): 494 (M<sup>+</sup>) (8.62), 148 (100). Anal. Calcd. for C<sub>24</sub>H<sub>22</sub>N<sub>4</sub>O<sub>4</sub>S<sub>2</sub> (494.59): C, 58.28; H, 4.48; N, 11.33. Found: C, 58.51; H, 4.69; N, 11.60.

**N-(3-Ethylphenyl)-2-((4-oxo-3-(4-sulfamoylphenyl)-3,4-dihydroquinazolin-2-yl)thio) acetamide (10)**

**10:** Yield, 73%; m.p. 197.6°C. IR: 3321, 3245, 3220 (NH<sub>2</sub>, NH), 3064 (arom.), 2973, 2837 (aliph.), 1689, 1662 (2CO), 1610 (CN), 1373, 1161 (SO<sub>2</sub>). <sup>1</sup>HNMR: 1.17 (t, 3H, *J* = 8.5 Hz), 2.59 (q, 2H, *J* = 8 Hz), 4.15 (s, 2H), 6.91 (ddd, 1H, *J* = 7 & 1.5 Hz), 7.22 (dd, 1H, *J* = 7 & 6 Hz), 7.43–7.50 (m, 2H), 7.60–7.64 (m, 3H), 7.75 (d, 2H, *J* = 7.5 Hz, AB), 7.84 (dd, 1H, *J* = 5.5 & 2 Hz), 8.07 (d, 2H, *J* = 7.5 Hz, AB), 8.11 (s, 2H), 10.29 (s, 1H). <sup>13</sup>CNMR: 15.95, 28.71, 37.83, 117.11, 117.30, 119.01, 119.19, 119.97, 123.49, 123.84, 126.48, 126.65, 127.51, 129.14, 129.20, 130.83, 135.55, 138.96, 139.11, 144.83, 145.94, 156.57, 161.08, 165.03. MS *m/z* (%): 494 (M<sup>+</sup>) (32.18), 155 (100).



Anal. Calcd. for  $C_{24}H_{22}N_4O_4S_2$  (494.59): C, 58.28; H, 4.48; N, 11.33. Found: C, 57.98; H, 4.21; N, 11.02.

**N-(4-Ethylphenyl)-2-((4-oxo-3-(4-sulfamoylphenyl)-3,4-dihydroquinazolin-2-yl)thio) acetamide (11)**

**11:** Yield, 89%; m.p. 259.4°C. IR: 3446, 3383, 3213 ( $NH_2$ , NH), 3062 (arom.), 2960, 2920 (aliph.), 1701, 1658 (2CO), 1606 (CN), 1336, 1161 ( $SO_2$ ).  $^1H$ NMR: 1.16 (t, 3H,  $J$  = 8.5 Hz), 2.52 (q, 2H,  $J$  = 8.0 Hz), 4.12 (s, 2H), 7.13 (d, 2H,  $J$  = 9 Hz, AB), 7.15–7.50 (m, 3H), 7.58–7.71 (m, 2H), 7.83 (d, 2H,  $J$  = 8 Hz, AB), 8.02 (dd, 1H,  $J$  = 6.5 Hz,  $J$  = 2 Hz), 8.08 (d, 2H,  $J$  = 8 Hz, AB), 8.09 (s, 2H), 10.36 (s, 1H).  $^{13}C$ NMR: 16.16, 28.05, 37.79, 119.68, 119.95 (4), 126.46, 126.64, 127.09, 127.39 (2), 128.45 (2), 130.67, 135.58, 137.10, 138.72, 146.78, 147.58, 156.69, 161.08, 165.78. MS  $m/z$  (%): 494 ( $M^+$ ) (63.34), 118 (100). Anal. Calcd. for  $C_{24}H_{22}N_4O_4S_2$  (494.59): C, 58.28; H, 4.48; N, 11.33. Found: C, 58.52; H, 4.64; N, 11.64.

**N-(4-Methoxyphenyl)-2-((4-oxo-3-(4-sulfamoylphenyl)-3,4-dihydroquinazolin-2-yl)thio) acetamide (12)**

**12:** Yield, 83%; m.p. 267.3°C. IR: 3367, 3313, 3291 ( $NH_2$ , NH), 3089 (arom.), 2972, 2844 (aliph.), 1694, 1668 (2CO), 1610 (CN), 1334, 1161 ( $SO_2$ ).  $^1H$ NMR: 3.71 (s, 3H), 4.11 (s, 2H), 6.88 (dd, 2H,  $J$  = 7 Hz, AB), 7.49 (dd, 2H,  $J$  = 7 Hz, AB), 7.51–7.62 (m, 3H), 7.75 (d, 2H,  $J$  = 6.5 Hz, AB), 7.85 (dd, 1H,  $J$  = 8.5 & 2 Hz, AB), 8.04 (d, 2H,  $J$  = 6.5 Hz, AB), 8.10 (s, 2H), 10.24 (s, 1H).  $^{13}C$ NMR: 27.91, 55.62, 114.38 (2), 119.95, 126.47 (2), 126.67 (2), 127.10 (2), 127.48, 130.85 (2), 132.49 (2), 135.61, 139.11, 145.89, 155.84, 156.59, 161.08, 165.47. MS  $m/z$  (%): 496 ( $M^+$ ) (15.66), 339 (100). Anal. Calcd. for  $C_{23}H_{20}N_4O_5S_2$  (496.56): C, 55.63; H, 4.06; N, 11.28. Found: C, 55.92; H, 4.29; N, 11.53.

**N-(4-Ethoxyphenyl)-2-((4-oxo-3-(4-sulfamoylphenyl)-3,4-dihydroquinazolin-2-yl)thio) acetamide (13)**

**13:** Yield, 90%; m.p. 262.4°C. IR: 3425, 3317, 3270 ( $NH_2$ , NH), 3100 (arom.), 2976, 2833 (aliph.), 1682, 1654 (2CO), 1618 (CN), 1396, 1163 ( $SO_2$ ).  $^1H$ NMR: 1.30 (t, 3H,  $J$  = 5 Hz), 3.97 (s, 2H), 4.11 (q, 2H,  $J$  = 4.5 Hz), 6.86 (d, 2H,  $J$  = 6.5 Hz, AB), 7.48 (dd, 2H,  $J$  = 6.5 Hz, AB), 7.49–7.61 (m, 3H), 7.76 (d, 2H,  $J$  = 6 Hz, AB), 7.85 (dd, 1H,  $J$  = 7.5 & 1.5 Hz, AB), 8.04 (d, 2H,  $J$  = 6 Hz, AB), 8.10 (s, 2H), 10.24 (s, 1H).  $^{13}C$ NMR: 15.14, 31.15, 63.55, 114.89 (2), 119.95, 121.19 (2), 126.47 (2), 126.67, 127.10, 127.48, 130.84 (2), 132.38, 135.60, 139.10,

145.92, 147.58, 155.11, 156.58, 161.09, 165.46. MS  $m/z$  (%): 510 ( $M^+$ ) (19.47), 316 (100). Anal. Calcd. for  $C_{24}H_{22}N_4O_5S_2$  (510.59): C, 56.46; H, 4.34; N, 10.97. Found: C, 56.19; H, 4.10; N, 10.62.

**N-(3,5-Dimethoxyphenyl)-2-((4-oxo-3-(4-sulfamoylphenyl)-3,4-dihydroquinazolin-2-yl)thio) acetamide (14)**

**14:** Yield, 92%; m.p. 283.7 °C. IR: 3450, 3366, 3170 ( $NH_2$ , NH), 3097 (arom.), 2927, 2831 (aliph.), 1687, 1655 (2CO), 1602 (CN), 1336, 1159 ( $SO_2$ ).  $^1H$ NMR: 3.70 (s, 6H), 4.10 (s, 2H), 6.22 (dd, 1H,  $J$  = 2.5 & 1.5 Hz), 6.89 (dd, 2H,  $J$  = 2.5 & 1.5 Hz), 7.47 (dd, 1H,  $J$  = 5.5 & 2.5 Hz), 7.55–7.59 (m, 2H), 7.83 (d, 2H,  $J$  = 9 Hz, AB), 7.95 (dd, 1H,  $J$  = 5.5 & 2.5 Hz), 8.07 (m, 4H), 8.09 (s, 1H).  $^{13}C$ NMR: 37.83, 55.55 (2), 95.92, 97.95 (2), 119.96 (3), 126.46, 126.56, 127.04, 129.89 (2), 135.49 (2), 141.19 (2), 147.58, 157.02, 160.95 (2), 161.12, 166.25. MS  $m/z$  (%): 526 ( $M^+$ ) (2.94), 276 (100). Anal. Calcd. for  $C_{24}H_{22}N_4O_6S_2$  (526.58): C, 54.74; H, 4.21; N, 10.64. Found: C, 54.47; H, 4.01; N, 10.37.

**2-((4-Oxo-3-(4-sulfamoylphenyl)-3,4-dihydroquinazolin-2-yl)thio)-N-(3,4,5-trimethoxyphenyl) acetamide (15)**

**15:** Yield, 86%; m.p. 267.6°C. IR: 3315, 3224, 3113 ( $NH_2$ , NH), 3072 (arom.), 2926, 2841 (aliph.), 1689, 1660 (2CO), 1610 (CN), 1342, 1165 ( $SO_2$ ).  $^1H$ NMR: 3.61 (s, 6H), 3.72 (s, 3H), 4.12 (s, 2H), 6.99 (d, 2H,  $J$  = 1.5 Hz), 7.49 (dd, 1H,  $J$  = 7.5 & 2 Hz), 7.50–7.61 (m, 2H), 7.76 (d, 2H,  $J$  = 6 Hz, AB), 7.85 (dd, 1H,  $J$  = 7.5 & 2 Hz), 8.05 (d, 2H,  $J$  = 6 Hz, AB), 8.10 (s, 2H), 10.30 (s, 1H).  $^{13}C$ NMR: 31.17, 56.12 (2), 60.56, 97.20 (2), 119.96 (3), 126.49, 126.69, 127.11, 127.46 (2), 130.84, 133.91, 135.55, 135.60, 139.04, 146.02, 153.20 (2), 156.58, 161.06, 165.85. MS  $m/z$  (%): 556 ( $M^+$ ) (12.43), 360 (100). Anal. Calcd. for  $C_{25}H_{24}N_4O_7S_2$  (556.61): C, 53.95; H, 4.35; N, 10.07. Found: C, 53.58; H, 4.09; N, 9.84.

**N-(2-Methyl-4-nitrophenyl)-2-((4-oxo-3-(4-sulfamoylphenyl)-3,4-dihydroquinazolin-2-yl)thio) acetamide (16)**

**16:** Yield, 76%; m.p. 255.8°C. IR: 3409, 3345, 3183 ( $NH_2$ , NH), 3100 (arom.), 2972, 2848 (aliph.), 1680, 1647 (2CO), 1620 (CN), 1538, 1343 ( $NO_2$ ), 1398, 1163 ( $SO_2$ ).  $^1H$ NMR: 2.29 (s, 3H), 4.25 (s, 2H), 7.49 (dd, 1H,  $J$  = 7 Hz & 1 Hz), 7.51–7.58 (m, 2H), 7.76 (d, 2H,  $J$  = 6.5 Hz, AB), 7.83–8.10 (m, 6H), 8.11 (s, 2H), 10.23 (s, 1H).  $^{13}C$ NMR: 18.32, 37.33, 115.34, 117.49, 120.00, 121.78 (2), 122.32,

123.72, 124.96, 125.97, 129.80 (2), 131.76, 134.27, 135.36, 136.28, 142.81, 143.21, 147.54, 156.56, 161.69, 166.81. MS  $m/z$  (%): 525 ( $M^+$ ) (18.53), 118 (100). Anal. Calcd. for  $C_{23}H_{19}N_5O_6S_2$  (525.56): C, 52.56; H, 3.64; N, 13.33. Found: C, 52.85; H, 3.93; N, 13.64.

**N-(2-Methyl-6-nitrophenyl)-2-((4-oxo-3-(4-sulfamoylphenyl)-3,4-dihydroquinazolin-2-yl)thio) acetamide (17)**

**17:** Yield, 80%; m.p. 246.5°C. IR: 3450, 3381, 3151 ( $NH_2$ , NH), 3095 (arom.), 2922, 2858 (aliph.), 1695, 1658 (2CO), 1616 (CN), 1541, 1339 ( $NO_2$ ), 1342, 1161 ( $SO_2$ ).  $^1H$ NMR: 2.29 (s, 3H), 4.18 (s, 2H), 7.36 (dd, 1H,  $J=7.5$  & 6 Hz), 7.51 (dd, 1H,  $J=7$  & 1.5 Hz), 7.58 (dd, 1H,  $J=7.5$  & 3 Hz), 7.59–7.74 (m, 2H), 7.76 (d, 2H,  $J=8.5$  Hz, AB), 7.88 (dd, 1H,  $J=7$  & 1.5 Hz), 8.04 (d, 2H,  $J=8.5$  Hz, AB), 8.10 (dd, 1H,  $J=6$  & 3 Hz), 8.11 (s, 2H), 9.0 (s, 1H).  $^{13}C$ NMR: 18.35, 36.76, 119.94, 122.61 (2), 126.59 (2), 126.71 (2), 127.02, 127.49, 130.85 (2), 135.32 (2), 135.56 (2), 137.61, 139.07, 145.95, 156.33, 161.14, 166.31. MS  $m/z$  (%): 525 ( $M^+$ ) (20.56), 324 (100). Anal. Calcd. for  $C_{23}H_{19}N_5O_6S_2$  (525.56): C, 52.56; H, 3.64; N, 13.33. Found: C, 52.19; H, 3.28; N, 13.07.

**N-(2,4-Dinitrophenyl)-2-((4-oxo-3-(4-sulfamoylphenyl)-3,4-dihydroquinazolin-2-yl)thio) acetamide (18)**

**18:** Yield, 74%; m.p. 277.8°C. IR: 3428, 3361, 3313 ( $NH_2$ , NH), 3100 (arom.), 2927, 2866 (aliph.), 1688, 1678 (2CO), 1606 (CN), 1537, 1345 ( $NO_2$ ), 1338, 1138 ( $SO_2$ ).  $^1H$ NMR: 4.18 (s, 2H), 7.46 (dd, 1H,  $J=8$  & 1.5 Hz), 7.61–7.72 (m, 2H), 7.73 (d, 2H,  $J=8.5$  Hz, AB), 7.82–8.04 (m, 3H), 8.06 (s, 2H), 8.10–8.62 (m, 3H), 9.91 (s, 1H).  $^{13}C$ NMR: 36.23, 119.10, 119.92, 120.29 (2), 121.07, 123.61, 124.80, 125.15, 128.82 (2), 129.40, 130.62, 133.71, 134.64, 136.07, 141.47, 142.72, 145.32, 160.61, 161.80, 167.92. MS  $m/z$  (%): 556 ( $M^+$ ) (32.82), 385 (100). Anal. Calcd. for  $C_{22}H_{16}N_6O_8S_2$  (556.53): C, 47.48; H, 2.90; N, 15.10. Found: C, 47.18; H, 2.63; N, 14.75.

## Antimicrobial Activity

The in-vitro antimicrobial activity screening was accomplished at the bacteriology laboratory, Botany and Microbiology Department, Faculty of Science, Al-Azhar University, Cairo, Egypt. The selected strains were; the Gram-positive *Bacillus subtilis* (ATCC 6633), *Staphylococcus aureus* (ATCC 29213), the Gram-negative *Escherichia coli* (ATCC 25922), *Pseudomonas aeruginosa* (ATCC 27853), MRSA and *Candida albicans* (ATCC

10231). The antimicrobial potential of the target compounds was measured as the diameter of the inhibition zones using the agar plate diffusion method.<sup>39</sup> Briefly, 100  $\mu$ L of the microorganism was grown in 10 mL of fresh media until they reached a count of  $10^8$  cells/mL for bacteria or  $10^5$  cells/mL for fungi. The count of microbial suspension was determined by a serial dilution which is defined as a series of sequential dilutions used to reduce a dense culture of cells to a more usable concentration. Each dilution will reduce the concentration of bacteria by a specific amount. One mL of each compound (at 0.5 mg/mL) was added to each well (10 mm diameter holes cut in the agar gel). The plates were incubated for 24 hrs at 37°C (for bacteria) and 72 hrs at 27°C (for yeast), each test was imitated three times. Tetracycline, ciprofloxacin and vancomycin were used as standard antibacterial reference drugs, while amphotericin B was used as the antifungal. The inhibition zone diameter was measured in millimeters and used as a criterion for the antimicrobial activity. Solvent control (DMSO) was included in every experiment as a negative control. The conventional paper disk diffusion method was used in measuring the MIC of the targeted compounds by applying paper disk (266,812 W. Germany 12.7 mm in diameter). Bacteria and yeast were grown on nutrient and Sabouraud agar medium, respectively. The compounds were loaded on paper disks with different concentrations. Dried disks were loaded on the surface of agar plates inoculated with the tested organism. Growth inhibition was examined after 24 hrs at 37°C for bacteria & 72 hrs at 27°C for yeast. Each test was replicated three times.<sup>35,40-42</sup>

## Synthesis and Characterization of 16-CuONPs Synthesized Using Gamma Irradiation

Gamma ( $\gamma$ ) irradiation was performed at the National Center for Radiation Research and Technology (NCRRT), Cairo, Egypt, using  $^{60}Co$ -Gamma chamber 4000 A-India operating at a dose rate of 1.221 KGy/h. Compound **16** was conjugated with CuONPs by adding **16** to 4.0 mM of copper sulfate pentahydrate solution in a ratio of 1:5 (v/v) with 0.2% isopropanol as a free radical scavenger. The solution was irradiated at different doses of gamma radiation as 1.0, 1.5, 2.0, 2.5, 3.0, 3.5, 4.0, 4.5 and 5.0 kGy. Characterization of the 16-CuONPs was performed by UV-Visible spectrophotometer using a filtrate (contains **16** only) as a baseline blank. Size distribution and average particle size were determined by Dynamic Light Scattering DLS-PSS-NICOMP 380-ZLS particle sizing system (St. Barbara, California, USA). The size and morphology of 16-CuONPs were recorded using the TEM model JEOL electron microscopy

JEM-100 CX. Drop coating 16-CuONPs prepared TEM studies onto carbon-coated TEM grids. X-Ray Diffraction patterns were obtained with The XRD-6000 series, including the residual austenite quantitation, stress analysis, crystallinity calculation, and crystallite size/lattice strain materials analysis by overlaying X-ray diffraction patterns using Cu-K $\alpha$  target, and nickel filter Shimadzu Scientific Instruments (SSI, Tokyo, Japan).

### Synthesis and Characterization of Compound 16 Nanoformulations (Chitosan Nanoparticles 16-CNPs and 16-CuONPs-CNPs)

CNPs were prepared by the ionotropic gelation method<sup>43</sup> through the electrostatic interactions between the amine group of chitosan and the negatively charged group of Triphenyl phosphate (TPP) as a polyanion. CS was dissolved in di-distilled water (DDW) to form a stock solution of concentration 0.5% (w/v) containing 1.2% acetic acid. During the process, CS undergoes ionotropic gelation and form spherical particles that are distinguishable by the opalescence of the solution. The lyophilized compound (50 mg) was mixed with 100 mL of CS solution 0.1% (w/v) to prepare drug-loaded chitosan nanoparticles. TPP 0.1% (w/v) was added dropwise to the compound/CS mixture with stirring for 10 min. Then, the solution was centrifuged (25,000  $\times$  g, 25°C for 30 min). The 16-CuONPs-CNPs were synthesized by loading compound 16 and CuONPs into chitosan through encapsulation.

The Zeta Sizer (Malvern Instruments, Worcestershire, UK) is used to measure the particle size, size distribution (polydispersity index (PDI)), and zeta potential of nanoparticles. The mean particle size was approximated as the z-average diameter and the width of the distribution as the PDI. DLS measurements were taken at 25°C with a detection angle of 90°. All measurements were calculated as the mean  $\pm$  standard deviation. Examination of the surface morphology and size distribution was performed by a transmission electron microscope (TEM) (JEOL electron microscopy JEM-100 CX). About 5  $\mu$ L of the nanoparticle solution was placed on a copper grid and stained with 2% (w/v) phosphotungstic acid.

### Evaluating Minimum Bactericidal Concentration (MBC)

MBC assay was conducted using the broth microdilution assay. The MBC was determined by plating 10  $\mu$ L of culture volume from the MIC assay onto trypticase soy broth (TSB) plate and colony formation was examined after 24 hrs. at 37°C. MBC is defined as the lowest

compound concentration resulting in a  $\cong$  3-log reduction in the number of colony-forming units (CFU).<sup>44</sup>

### In vitro Inhibitory Activity Screening on *Staphylococcus aureus* DNA Gyrase

The supercoiling assay was carried out according to the manufacturer's instructions.<sup>45</sup> Briefly, set up a mix of assay buffer (6  $\mu$ L of 5x buffer), relaxed pBR322 (0.5  $\mu$ L) and water (17.5  $\mu$ L) on ice. Add the aliquot 24  $\mu$ L of the mix into tubes. Add 3  $\mu$ L of DMSO to tubes 1 and 2. Add 3  $\mu$ L of the tested compound to the other tubes then mix briefly. Add 3  $\mu$ L of dilution buffer to tube 1. Dilute the enzyme in dilution buffer then add 3  $\mu$ L of this to the remaining tubes. Mix and incubate for 30 mins at 37°C. Stop the reaction then centrifuge for 1 min. Load 20  $\mu$ L of aqueous (upper blue) phase onto a 1% (w/v) agarose gel. Run at 75 V for approximately 2 hrs. Stain with 1  $\mu$ g/mL ethidium bromide in water (15 mins), destains (5–10 mins) in water. Measurement of the concentration of the compound required for 50% inhibition of enzyme activity (IC<sub>50</sub>) was performed using GraphPad Prism 5 software and the results represent the mean of three independent measurements.

### MTT Assay

The 96 well tissue culture plate was inoculated with 10<sup>5</sup> cells/mL (100  $\mu$ L/well) and incubated at 37°C for 24 hrs. Two-folds dilutions of the tested sample were made in maintenance medium with 2% serum. A 0.1 mL of each dilution was tested. MTT solution was prepared (5mg/mL in phosphate-buffered saline (PBS)) (Bio Basic Canada Inc.) and 20  $\mu$ L was added to each well. Incubate at 37 °C and 5% CO<sub>2</sub> for 1–5 h. Resuspend formazan in 200  $\mu$ L DMSO. Optical density was measured at 560 nm and the IC<sub>50</sub> was calculated using Graphpad prism 5.

### Molecular Docking

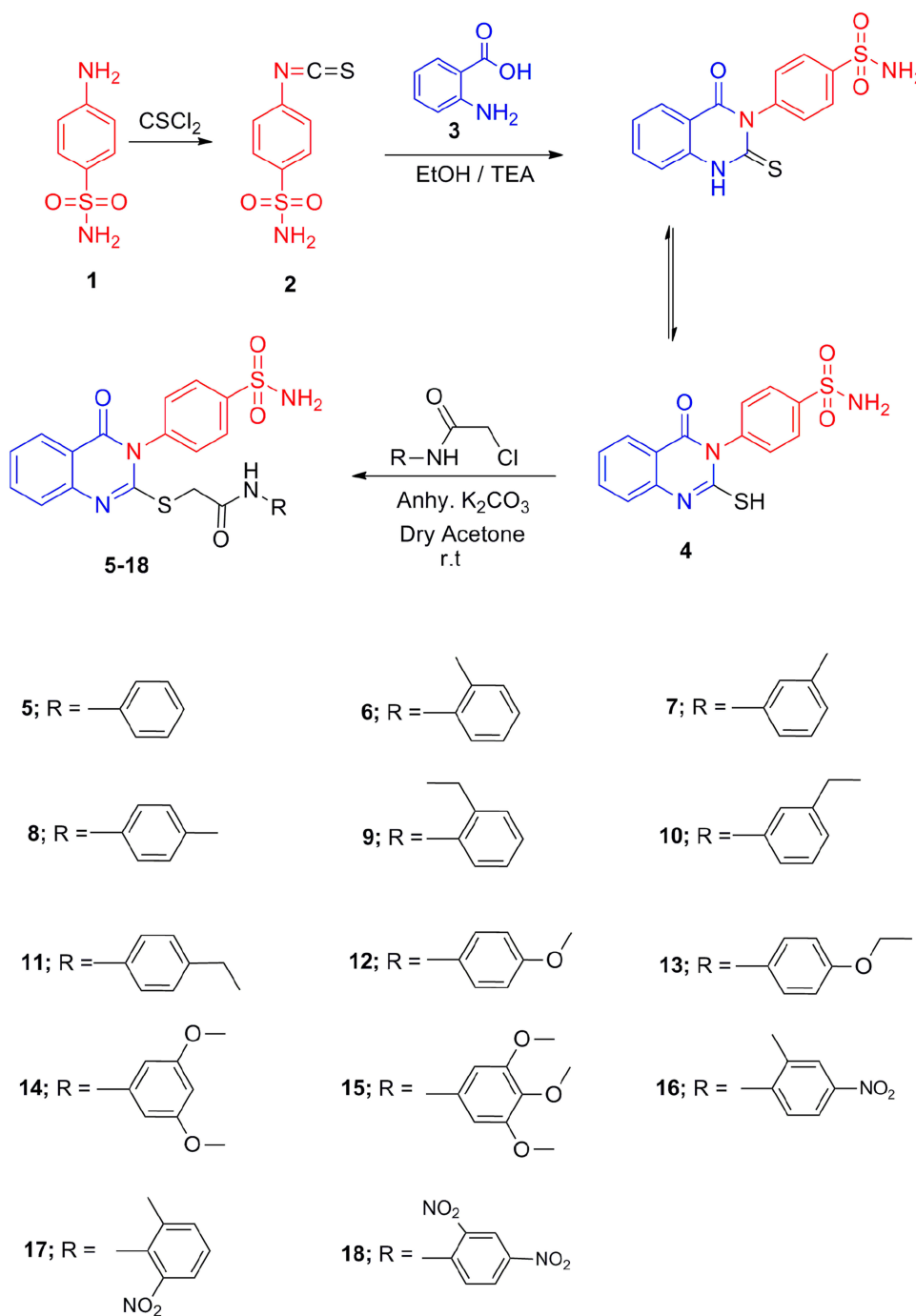
The docking study was performed using MOE 10.2008 software. The PDB file containing *S. aureus* DNA gyrase co-crystallized with ciprofloxacin was obtained from the protein data bank (PDB: 2XCT). Water molecules were ignored and hydrogen atoms were added. Alpha Site Finder was used to detect the active site in the enzyme. Energy minimizations were performed with an RMSD gradient of 0.001 kcal mol<sup>-1</sup>Å<sup>-1</sup> and MMFF94X force field. Ciprofloxacin was removed from the active site and then re-docked again giving

energy score ( $S$ ) =  $-8.34 \text{ kcal mol}^{-1}$  and RMSD of  $1.55 \text{ \AA}$  followed by the docking of compound **16**. The validated docking protocol was then used to study the ligand–target interactions in the active site to predict the binding mode and rationalize the biological activity results.

## Results and Discussion

### Chemistry

**Scheme 1** shows the synthetic pathways adopted for the development of the quinazolinone benzenesulfonamide derivatives **5–18**. The starting material 4-(2-mercapto-4-oxoquinazolin-3(4*H*)-yl) benzenesulfonamide **4** was prepared from



**Scheme 1** | Synthesis of the quinazolinone benzenesulfonamide derivatives **4–18**.



the reaction of 4-isothiocyanatobenzenesulfonamide **2**<sup>46</sup> and anthranilic acid **3**. Coupling of **4** with the 2-chloro-*N*-substituted acetamide in dry acetone and anhydrous K<sub>2</sub>CO<sub>3</sub> yielded the corresponding 2-((4-oxo-3-(4-sulfamoylphenyl)-3,4-dihydroquinazolin-2-yl)thio)-*N*-substituted acetamides **5–18**. IR spectra of **5–18** displayed NH, CH<sub>2</sub> aliphatic and CO bands at their assigned regions. <sup>1</sup>H-NMR spectra of **5–18** revealed two singlets, one at the range of 3.97 to 4.30 ppm referring to the CH<sub>2</sub> and the other at 8.09 to 10.40 ppm attributed to the NH acetamide protons. <sup>13</sup>C-NMR of **5–18** exhibited two signals peculiar to the CH<sub>2</sub> and CO carbons. <sup>1</sup>H-NMR spectra of **6–8** showed singlets at 2.20, 2.24 and 2.08 ppm assigned to the CH<sub>3</sub> group at the *ortho*, *meta* and *para*- positions of the phenyl ring, respectively. <sup>13</sup>C-NMR of **6–8** showed signals at 18.32, 20.90 and 22.13 ppm for the CH<sub>3</sub> groups. <sup>1</sup>H-NMR spectra of **9–11** revealed triplets at 1.06, 1.17 & 1.16 ppm attributed to the CH<sub>3</sub> ethyl, and quartet at 2.58, 2.59 and 2.52 ppm referring to the CH<sub>2</sub> ethyl at the *ortho*, *meta* and *para*- positions. <sup>13</sup>C-NMR of **9–11** showed two signals at 14.64, 15.95 & 16.16 ppm assigned to CH<sub>3</sub> ethyl and 24.13, 28.71 & 28.05 ppm due to the CH<sub>2</sub> ethyl groups, respectively. The <sup>1</sup>H-NMR spectrum of **12** revealed a singlet at 3.71 ppm attributed to the OCH<sub>3</sub> protons, while <sup>13</sup>C-NMR of **12** showed a signal at 55.62 ppm due to the OCH<sub>3</sub> carbon. The <sup>1</sup>H-NMR spectrum of **13** revealed triplet at 1.30 ppm and quartet at 4.11 ppm due to the ethoxy group. The <sup>1</sup>H-NMR spectrum of **14** revealed a singlet at 3.70 ppm attributed to the 2OCH<sub>3</sub> protons, while **15** revealed two singlets at 3.61 and 3.72 ppm due to the 3OCH<sub>3</sub> protons. IR spectra of **16–18** showed bands of NO<sub>2</sub> groups at their specified regions. <sup>1</sup>H-NMR spectra of **16** and **17** showed singlet at 2.29 ppm assigned to the CH<sub>3</sub>, while <sup>13</sup>C-NMR of **16** and **17** showed a signal at 18.32 and 18.35 ppm attributed to the CH<sub>3</sub> group.

## Antimicrobial Activity

The synthesized compounds **4–18** were evaluated for their in vitro antibacterial potential against *Bacillus subtilis* and *Staphylococcus aureus* as examples of Gram-positive bacteria, *Escherichia coli* and *Pseudomonas aeruginosa* as examples of Gram-negative bacteria, Methicillin-resistant *Staphylococcus aureus* (MRSA) and antifungal potential against *Candida albicans* as unicellular fungi. As depicted in Table 1, the synthesized compounds **4–18** displayed potent antibacterial and antifungal activities. Compound **16** was the most potent in this series against both the bacterial and fungal strains and showed the highest inhibitory activity against the Gram-positive strains.

Compound **16** showed larger inhibition zone (IZ) than that of tetracycline, ciprofloxacin, vancomycin and amphotericin B, with minimum inhibitory concentration (MIC) lower than that of tetracycline ciprofloxacin, vancomycin and amphotericin B except for MRSA, compound **16** MIC was higher than that of ciprofloxacin and vancomycin (MIC= 5.0 µg/mL versus 1.25 and 3.90 µg/mL, respectively). Regarding the antibacterial activity \_in terms of the inhibition zone\_ the 2-methyl-4-nitrophenyl, the 4-ethoxyphenyl and the 2-methyl-6-nitrophenyl derivative (**16**, **13** & **17**) were the most potent compounds against Gram-positive bacteria and showed larger IZ than that of tetracycline, ciprofloxacin and vancomycin. Compounds **5**, **8**, **11**, **13**, **16–18** displayed better activity against Gram-positive bacteria compared to tetracycline. While compounds **16** and **9** showed more potent activity against Gram-negative bacteria compared to the reference drugs. Regarding the antifungal activity, compounds **7**, **8**, **13**, **16–18** showed more potent or equipotent activity compared to amphotericin B. However, compounds **13**, **16** and **17** exhibited the most potent activity towards MRSA. The MICs of all compounds are listed in Table 1. It is apparent that the majority of compounds showed lower MIC than that of tetracycline but not ciprofloxacin. The MIC value for compound **16** ranges from 0.3 to 5 µg/mL against all the tested microorganisms.

## Synthesis and Characterization of Copper Oxide Nanoparticles (16-CuONPs)

Compound **16** was mixed with copper sulfate pentahydrate solution and was irradiated at different doses of gamma radiation as shown in Table 2. The CuONPs synthesized at different gamma radiation doses showed maximum absorption (2.322) at the wavelength of 445 nm, by 4.5 kGy. In this method, hydrated electrons were produced during gamma irradiation. Compound **16** acts as a stabilizing agent by reducing the copper ions to metal oxide nanoparticles.

Characterization of 16-CuONPs was performed through UV-Vis spectrum, Dynamic Light Scattering (DLS), Transmission Electron Microscopy (TEM) and X-Ray Diffraction pattern (XRD). Size distribution and average particle size together with the morphology of the synthesized 16-CuONPs were figured. The colloidal solution of CuONPs displayed an intense dark green color, as a result of spectra scattered and emitted through low dimensionality. Figure 2 displays the UV-visible spectrum of CuONPs synthesized by compound **16**. On the other hand, there is a slight shift in



**Table 1** The In Vitro Antimicrobial Activity of Compounds 4–18 Showing the Inhibition Zones (IZ) and Minimum Inhibition Concentration (MIC) Against the Selected Strains

Compound Code	Mean Diameter of Inhibition Zone (mm) and Minimal Inhibitory Concentrations (MIC)											
	B. subtilis (ATCC 6633)		S. aureus (ATCC 29,213)		E. coli (ATCC 25,922)		P. aeruginosa (ATCC 27,853)		C. albicans (ATCC 10,231)		MRSA	
	IZ	MIC	IZ	MIC	IZ	MIC	IZ	MIC	IZ	MIC	IZ	MIC
4	16 ± 0.01	2.50	13 ± 0.04	5.00	NA	–	NA	–	14 ± 0.05	2.50	NA	–
5	25 ± 0.07	2.50	22 ± 0.31	1.56	14 ± 0.23	10.00	15 ± 0.21	20.00	19 ± 0.05	5.00	20 ± 0.18	10.00
6	16 ± 0.10	15.63	14 ± 0.03	31.25	15 ± 0.31	5.00	17 ± 0.13	7.50	20 ± 0.25	3.91	NA	–
7	20 ± 0.21	1.25	15 ± 0.07	2.50	12 ± 0.15	20.00	14 ± 0.03	15.63	22 ± 0.08	10.00	10 ± 0.02	7.81
8	26 ± 0.16	6.31	23 ± 0.09	12.50	NA	–	NA	–	24 ± 0.16	6.31	19 ± 0.01	20.00
9	22 ± 0.16	2.50	18 ± 0.12	5.00	30 ± 0.28	1.25	25 ± 0.14	2.50	21 ± 0.14	5.00	14 ± 0.13	15.63
10	16 ± 0.04	7.81	12 ± 0.04	15.63	NA	–	NA	–	NA	–	NA	–
11	28 ± 0.13	1.25	26 ± 0.31	2.50	14 ± 0.14	5.00	16 ± 0.11	20.00	18 ± 0.19	10.00	22 ± 0.09	10.00
12	21 ± 0.20	1.95	24 ± 0.26	10.00	13 ± 0.12	10.00	15 ± 0.16	12.51	21 ± 0.05	7.81	20 ± 0.21	7.81
13	35 ± 0.14	0.49	33 ± 0.17	1.25	12 ± 0.17	1.25	14 ± 0.12	10.00	26 ± 0.30	5.00	28 ± 0.16	5.00
14	24 ± 0.02	2.50	27 ± 0.21	3.90	16 ± 0.01	5.00	20 ± 0.21	7.81	20 ± 0.21	6.31	24 ± 0.13	12.50
15	20 ± 0.04	7.81	16 ± 0.01	15.63	13 ± 0.04	15.63	18 ± 0.12	10.00	14 ± 0.11	3.80	12 ± 0.09	31.25
16	36 ± 0.11	0.31	35 ± 0.09	0.62	32 ± 0.20	1.25	25 ± 0.11	2.50	27 ± 0.12	1.25	29 ± 0.05	5.00
17	30 ± 0.20	1.25	28 ± 0.25	5.00	16 ± 0.23	5.00	11 ± 0.05	3.80	22 ± 0.20	10.00	25 ± 0.09	10.00
18	28 ± 0.17	2.50	26 ± 0.17	7.50	15 ± 0.12	7.50	13 ± 0.21	15.63	24 ± 0.27	3.13	23 ± 0.20	15.63
Tetracycline	25 ± 0.01	31.25	25 ± 0.04	62.50	23 ± 0.31	15.63	20 ± 0.10	62.50	–	–	–	–
Ciprofloxacin	29 ± 0.15	0.80	27 ± 0.23	0.78	27 ± 0.98	1.57	24 ± 0.47	3.13	–	–	22 ± 0.50	1.25
Vancomycin	21 ± 0.40	1.95	17 ± 0.11	1.57	24 ± 0.20	1.38	22 ± 0.85	2.50	–	–	14 ± 0.65	3.90
Amphotericin B	–	–	–	–	–	–	–	–	22 ± 0.11	15.63	–	–

**Notes:** NA indicates no activity. (–) indicates not tested. Each value represents the mean of three different experiments ± standard error. Tetracycline, ciprofloxacin and vancomycin were used as standards against the tested bacteria while Amphotericin B was used for fungi.

**Table 2** The Effect of Different Doses of Gamma Radiation (kGy) on CuONPs Synthesis

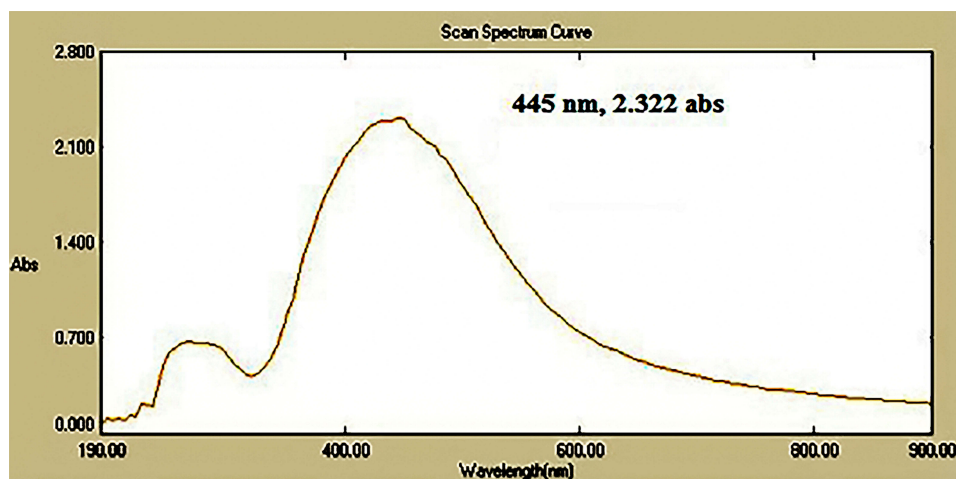
Radiation Doses (kGy)	Maximum Absorption (O.D)	Wavelength (nm)
Control (non-irradiated)	0.065	425
1.0	0.071	425
1.5	0.085	430
2.0	1.312	445
2.5	1.125	465
3.0	1.294	460
3.5	1.125	465
4.0	1.242	430
4.5	2.322	445
5.0	1.170	440

the UV–Vis peaks towards the small size. To monitor the particle size distribution, DLS was performed, and its results were compared with the TEM data. The average particle size determined by the DLS method<sup>47,48</sup> was found to be 36.3 nm in 16-CuONPs. On the other hand, the TEM result demonstrated spherical particles within a nanoscale range from

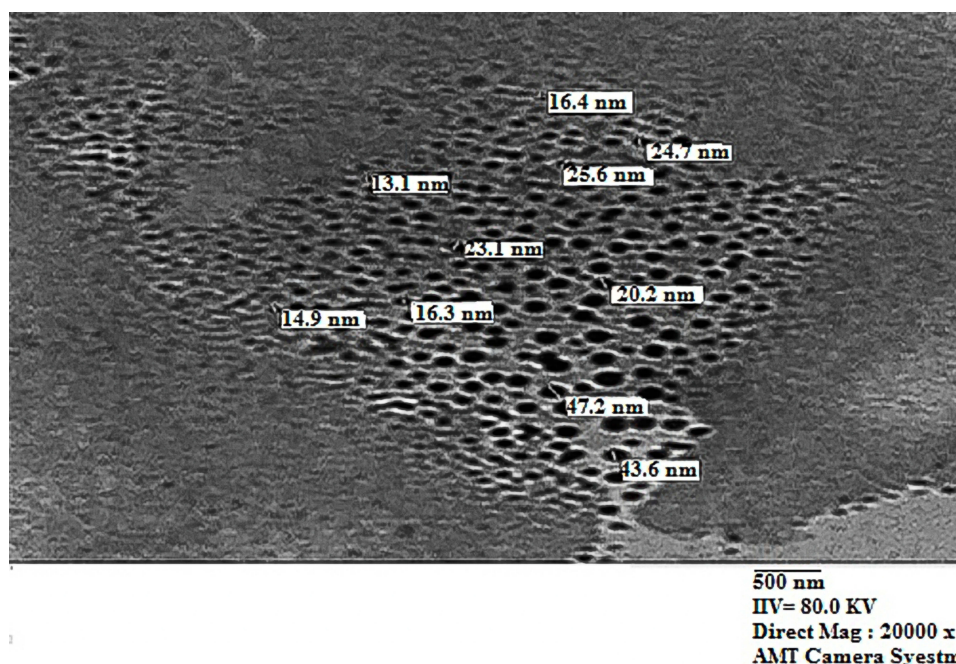
13.1 nm to 43.6 nm with the average main diameter of 25.31 nm as shown in Figure 3. The XRD allows better visualization of the crystal structure of the observed atoms because it shows axes, shape, size and position of the atoms. The XRD pattern for the copper aggregates is shown in Figure 4, several peaks were observed. Diffraction characteristics appeared at two-theta (degree) at 35.6° and 38.8°, corresponding to the (002) and (111) planes of CuONPs, respectively, matching the conventional powder diffraction card of the Joint Committee on Powder Diffraction Standards (JCPDS).<sup>49,50</sup>

#### Mechanistic Design for Gamma-Assisted Nucleation and Germination of 16-CuONPs (Radiolysis)

The Kinetic study of the reduction method confirmed that the construction of 16-CuONPs can start without the aid of radiation; but was exceedingly enhanced by gamma irradiation particularly at 4.5 kGy, implying that radiation has a significant role in the organization of 16-CuONPs. The radicals and electrons generated in water simultaneously by gamma irradiation are  $e^-_{aq}$ ,  $OH^\bullet$ ,  $H^\bullet$ ,  $H_2$ , and  $H_2O_2$  (Equ. 1). The success of



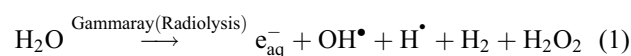
**Figure 2** The UV-visible spectrum of CuONPs synthesized by compound **16** using 4.5 KGy.



**Figure 3** TEM image of CuONPs synthesized by compound **16** using 4.5 KGy of gamma radiation.

gamma irradiation to form the 16-CuONPs extends the evidence that the target product of extremely reducing free electron was formed without the creation of another byproduct. The overall reaction was carried out by the use of the available electron as a reducing cause to  $\text{Cu}^{+2}$  ions and the effectiveness of compound **16** to act as a stabilizer towards CuONPs formation. The reaction started by dissolving  $\text{CuSO}_4$  into the water and its hydrolysis to its ions  $\text{Cu}^{+2}$  and  $\text{SO}_4^{-2}$  (Equ. 2). The conversion of  $\text{Cu}^{+2}$  takes place by electron removal from the hydrated electrons to create zerovalent  $\text{Cu}^0$

(Equ. 3). The free radicals  $\text{OH}^\bullet$  and  $\text{H}^\bullet$  are competent to discharge hydrogen from the *N*-(2-methyl-4-nitrophenyl)-2-((4-oxo-3-(4-sulfamoylphenyl)-3,4-dihydroquinazolin-2-yl)thio) acetamide **16**. Secondary radical was formed,  $\text{C}_{23}\text{H}_{19}\text{N}_5\text{S}_2\text{O}_6^\bullet$  (Equ. 4). Additionally, compound **16** radical used  $\text{Cu}^{+2}$  to form CuONPs (Equ. 5). Eventually, the stable active compound can preserve CuONPs as referred to in Equation 6.



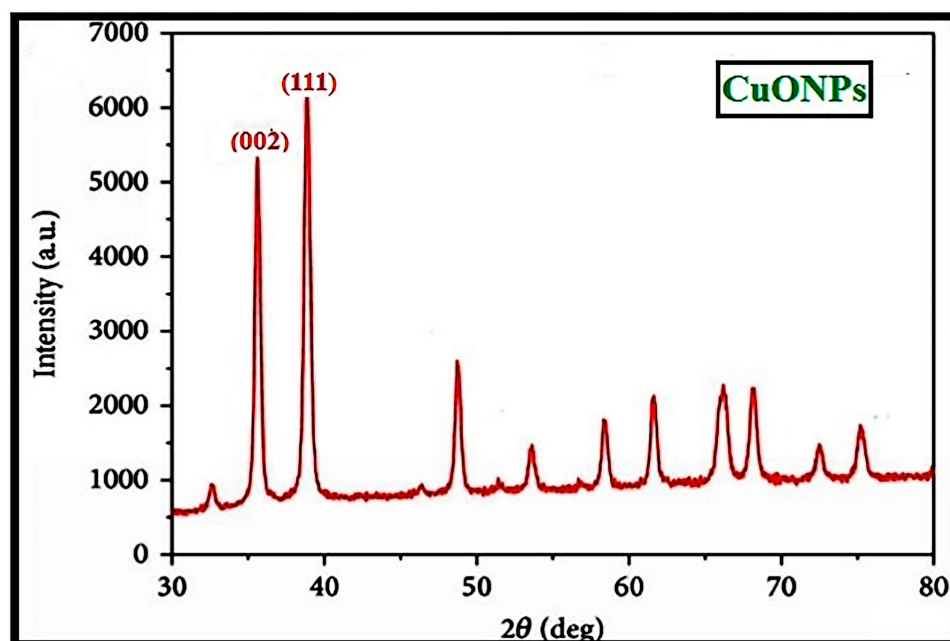
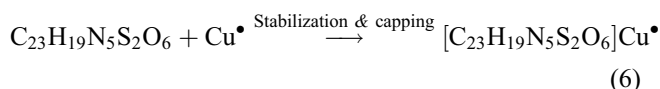
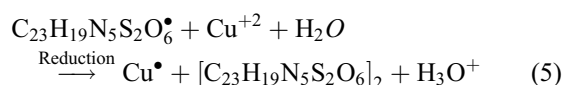
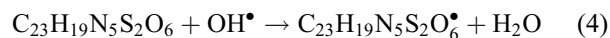
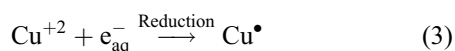
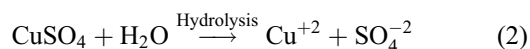


**Figure 4** XRD image of CuONPs synthesized by compound **16** using 4.5 KGy of gamma radiation.



### Synthesis of Compound **16** Nanoformulations

#### Synthesis and Characterization of Compound **16** Loaded Chitosan NPs (16-CNPs)

Compound **16**, the most potent against all the selected bacterial and fungal strains, was further chosen to be loaded on chitosan nanoparticles in order to determine the effect of nanoformulation on its antimicrobial potency. Chitosan nanoparticles were easily obtained by means of ionic gelation between cationic chitosan and anionic triphenyl phosphate (TPP) and were applied for the encapsulation of 16-CNPs. The zeta sizer analysis of the prepared NPs revealed that the loading of compound **16** led to an increase in the NPs average diameter, to be  $483.7 \pm 37.83$  nm in comparison to  $478.4 \pm 6.27$  nm for blank

CNPs. Both CNPs and 16-CNPs displayed positive Zeta potential values in SPB (sodium phosphate buffer) at pH 7.4, due to the cationic nature of chitosan. Compound **16** loading led to a decrease in the Zeta potential value from  $10.0 \pm 0.36$  to  $4.6 \pm 0.88$  mV (Table 3, Figures 5 & 6). The TEM examination of both CNPs and 16-CNPs demonstrated spherical shape (Figures 7 & 8).

#### Synthesis and Characterization of 16-CuONPs-CNPs Nanocomposites

The 16-CuONPs-CNPs were synthesized by loading compound **16** and CuONPs into chitosan through encapsulation to determine the effect of nanocomposite formation on the activity. The zeta sizer analysis demonstrated that the loading of compound **16** and CuONPs has led to an increase in the average diameter, to be  $304.3 \pm 83.42$  nm. Compound **16** and CuONPs loading led to a decrease of the Zeta potential

**Table 3** The Main Characteristics of the Nanoformulations: Average Size Distribution (Nm), Particles Diameter Index (Pdl) and Surface Charge (mV)

Formulation	Size (nm ± SD)	Pdl	Zeta Potential (mV ± SD)
CNPs	$478.8 \pm 6.27$	$0.502 \pm 0.069$	$10.0 \pm 0.36$
16-CNPs	$483.7 \pm 37.83$	$0.491 \pm 0.023$	$4.6 \pm 0.88$
16-CuONPs-CNPs	$304.3 \pm 83.42$	$0.424 \pm 0.068$	$4.7 \pm 0.58$

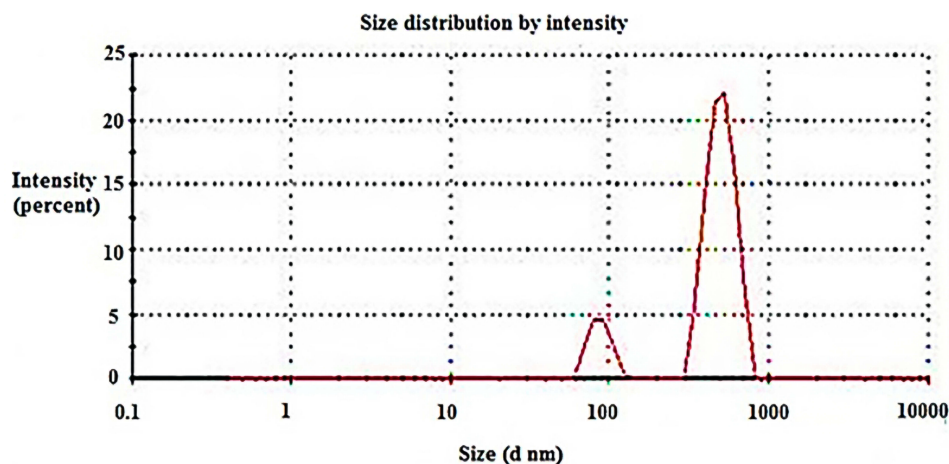


**Figure 5** Average size distribution of chitosan nanoparticles (CNPs).

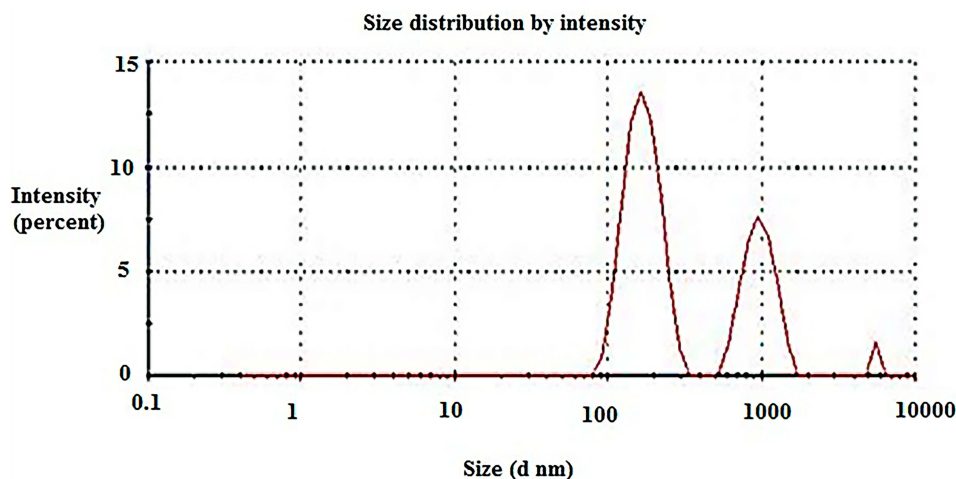


**Figure 6** Average size distribution of compound **16** loaded chitosan nanoparticles (16-CNPs).

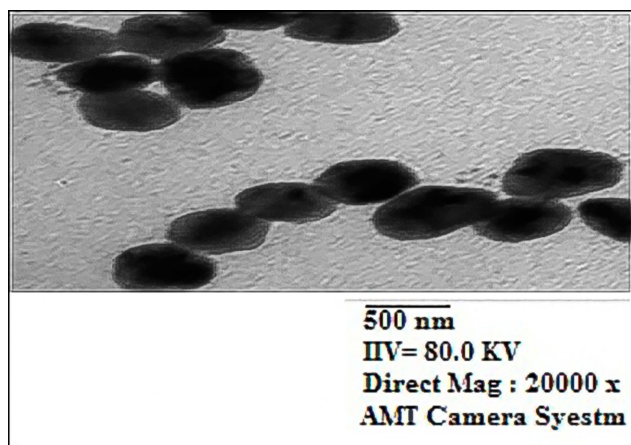


**Figure 7** TEM image of chitosan nanoparticles (CNPs).

values to be  $4.7 \pm 0.58$  mV (Table 3). The TEM demonstrated a spherical shape for these nanocomposites (Figures 9 & 10).

### Antimicrobial Evaluation of the Synthesized Nanoformulations

As mentioned before, CuONPs have broad-spectrum antimicrobial properties. So, compound **16** loaded CuONPs were synthesized and screened for antimicrobial activity and compared with that of CNPs and 16-CNPs. Table 4 shows the effect of different nanoformulations of compound **16** on its antimicrobial activity. It is obvious that chitosan itself possesses good antimicrobial activity and the same for compound **16** alone. However, the nano



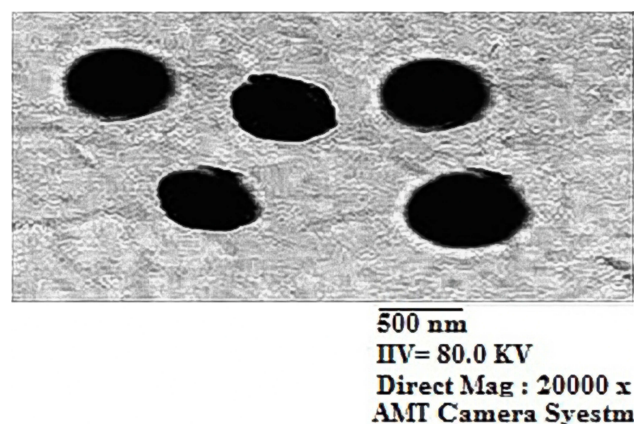


**Figure 8** TEM image of compound **16** loaded chitosan nanoparticles 16-CNPs.

formula 16-CNPs displayed better antimicrobial activity towards all the selected strains. The inhibition zones of the nano formula 16-CNPs range from 29 to 43 mm and the MIC from 0.07 to 2.50  $\mu\text{g/mL}$ . The antimicrobial activity of 16-CuONPs and 16-CuONPs-CNPs was also screened against the chosen strains. 16-CuONPs were found to exhibit moderate activity, while the nanocomposites 16-CuONPs-CNPs showed the most potent activity against all the selected strains. The 16-CuONPs-CNPs showed inhibition zones in the ranges of 34–45 mm and MIC in the range of 0.03–1.25  $\mu\text{g/mL}$ , which is more potent than that of ciprofloxacin (Figure 11). In order to further study and confirm whether the above promising nanoformulations were bactericidal or bacteriostatic the relationship between MBC and MIC was applied (Table 4). The antibacterial agents are generally regarded as bactericidal if the MBC is not more than four times the MIC.<sup>51</sup> By applying the MBC/MIC ratio it can be concluded that compound **16**

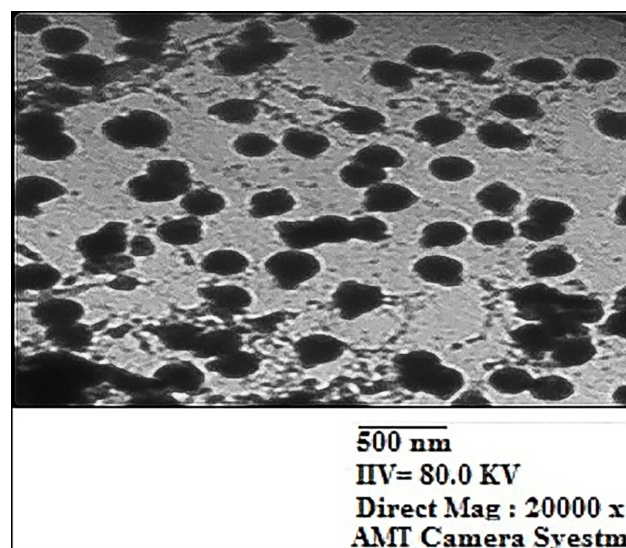


**Figure 10** TEM image of compound **16** loaded chitosan and copper oxide nanoparticles 16-CuONPs-CNPs.

and its nanoformulations exhibited bactericidal and fungicidal properties.

#### Evaluation of the DNA Gyrase Inhibitory Activity

DNA gyrase is a type II topoisomerase that is responsible for maintaining the correct level of supercoiling in bacterial DNA. It is essential in bacteria but is missing in higher eukaryotes. Ciprofloxacin is a fluoroquinolone broad-spectrum antibiotic owing to its DNA gyrase inhibitory effect. Compound **16** and the nanoformulations were screened for their inhibitory effect against *Staphylococcus aureus* DNA gyrase and showed  $\text{IC}_{50}$  values ranging from 10.57 to 27.32  $\mu\text{g/mL}$ . The nano formula 16-CuONPs-CNPs showed the highest activity

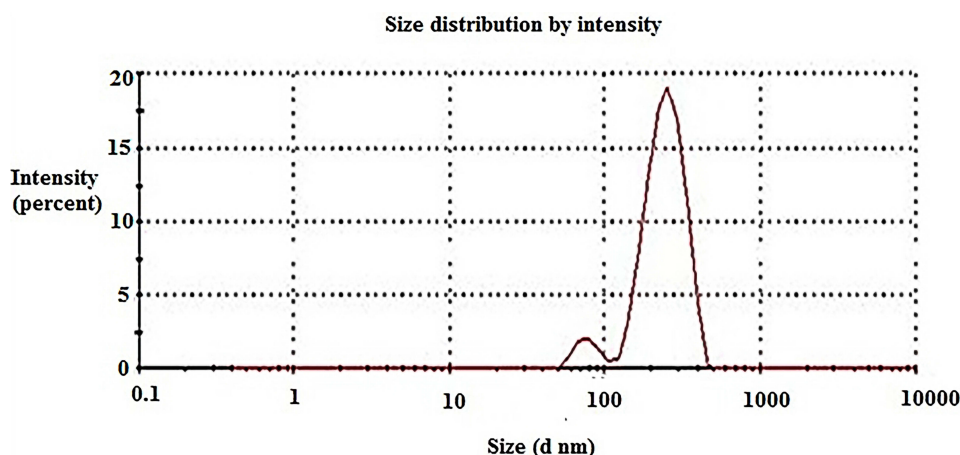


**Figure 9** Average size distribution of compound **16** loaded chitosan and copper oxide nanoparticles 16-CuONPs-CNPs.



Table 4 The Antimicrobial Activity of Compound 16 Nanoformulations

Microbial Test Strains	Mean Diameter of Inhibition zone (IZ)(mm)/Minimal Inhibitory Concentration (MIC) (μg/mL)/minimal bactericidal Concentration(μg/mL).														
	Compound 16			16-CuONPs			CNPs			16-CuONPs-CNPs			Ciprofloxacin		
	IZ	MIC	MBC	IZ	MIC	MBC	IZ	MIC	MBC	IZ	MIC	MBC	IZ	MIC	MBC
<i>B. subtilis</i> (ATCC 6633)	36±0.11	0.31	0.62	20±0.05	7.81	15.62	27±0.23	3.91	7.03	43±0.03	0.07	0.14	45±0.11	0.03	0.06
<i>S. aureus</i> (ATCC 29,213)	35±0.09	0.62	1.17	17±0.13	62.5	87.50	24±0.07	5.20	10.00	41±0.08	0.15	0.31	43±0.20	0.07	0.14
<i>E. coli</i> (ATCC 25,922)	32±0.20	1.25	2.50	14±0.07	15.62	24.99	22±0.11	7.81	14.05	35±0.22	0.31	0.62	39±0.13	0.15	0.31
<i>P. aeruginosa</i> (ATCC 27,853)	25±0.11	2.50	4.50	16±0.04	31.25	62.50	20±0.21	10.41	17.69	29±0.13	0.62	1.24	34±0.05	0.31	0.62
<i>C. albicans</i> (ATCC 10,231)	27±0.12	1.25	2.12	18±0.18	62.50	81.25	21±0.02	12.51	21.26	33±0.04	0.83	1.66	37±0.04	0.41	0.82
<i>S. aureus</i> (MRSA)	29±0.05	5.00	9.01	19±0.21	125.0	175.0	18±0.25	41.60	74.88	32±0.17	2.50	4.50	35±0.11	1.25	2.25

Notes: (-) indicates not tested. The results represent three independent experiments ± SE.

with  $IC_{50} = 10.57 \mu\text{g/mL}$  compared to ciprofloxacin  $IC_{50} = 8.72 \mu\text{g/mL}$ .

It is clear from the results in Table 5 that compound 16 ( $IC_{50} = 16.21 \mu\text{g/mL}$ ) showed more potent activity after being incorporated into nanoformulations; 16-CNPs ( $IC_{50} = 14.26 \mu\text{g/mL}$ ), 16-CuONPs ( $IC_{50} = 12.49 \mu\text{g/mL}$ ), and 16-CuONPs-CNPs. Also, chitosan NPs showed more potent inhibitory activity after being formulated with compound 16 to form 16-CNPs ( $IC_{50} = 27.32$  versus  $14.26 \mu\text{g/mL}$ ). Molecular docking was conducted to study the possible binding of 16 inside the active site of *S. aureus* DNA gyrase.

### Cytotoxicity Test

In order to determine the relative safety of compound 16, 16-CNPs and 16-CuONPs-CNPs, the cytotoxic effect on VERO cell line (ATCC CCL-81) was measured using the MTT assay.<sup>52</sup> Compound 16 showed the least cytotoxicity with an  $IC_{50}$  of  $927.28 \mu\text{g/mL}$  indicating its safety to normal cells. Also, 16-CNPs and 16-CuONPs-CNPs displayed a very low cytotoxic effect ( $IC_{50} = 543$  and  $637 \mu\text{g/mL}$ , respectively) (Table 6).

### Molecular Docking

*Staphylococcus aureus* DNA gyrase (PDB: 2XCT) consists of four lobes with four active sites in which ciprofloxacin binds. The DNA strands intercalate with ciprofloxacin-forming interactions with DNA structure.<sup>53</sup> The various substitutions on the quinazolinone ring can play an effective role in its binding to the receptor. The interaction energy and the binding mode of compound 16 were in agreement with that of ciprofloxacin. Ciprofloxacin binds inside the active site through two  $\pi$ - $\pi$  and cation- $\pi$  interactions to the DNA fragments DG:A9, DA:B13 and  $Mn^{2+}$  through its carboxylic group with binding energy  $S = -8.34 \text{ Kcal mol}^{-1}$  (Figure 12). Compound 16 was able to adopt the same binding mode as ciprofloxacin and establish the same contact with  $Mn^{2+}$  through its  $SO_2$  group, which is crucial for binding and forms cation- $\pi$  interaction with Arg A1033, hydrogen bonds with Ser A1084 of binding energy  $S = -8.82 \text{ Kcal mol}^{-1}$  (Figure 13). Superimposition of ciprofloxacin & compound 16 showed that both adopt the same orientation directed towards  $Mn^{2+}$  by the carboxylic &  $SO_2$  groups, respectively (Figure 14 & Table 7).

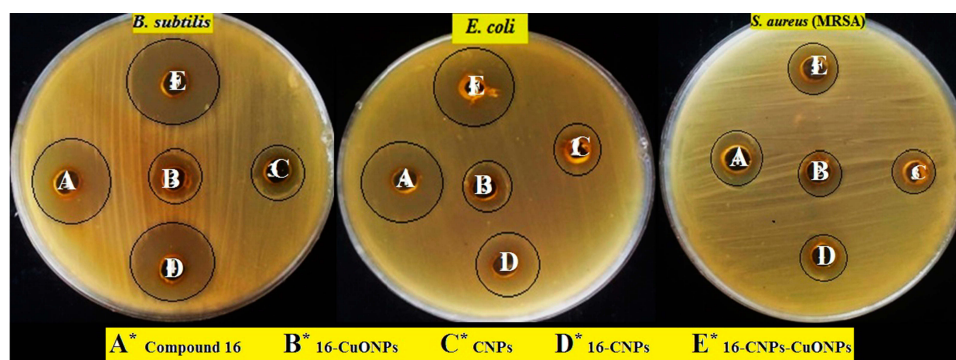


**Figure 11** Inhibition zones of compound **16** and its nanoformulations, A: Compound **16**, B: 16-CuONPs, C: CNPs, D: 16-CNPs and E: 16-CuONPs-CNPs.

## Conclusion

Novel quinazolinone benzenesulfonamide derivatives **4–18** were synthesized and screened for their antimicrobial activity against Gram-positive bacteria, Gram-negative bacteria, MRSA and yeast. The 2-methyl-4-nitrophenyl derivative **16** was the most potent against the selected strains and showed inhibition zones and MIC in the ranges of 25–36 mm and 0.31–5.0 µg/mL, respectively. The most potent activity was against the Gram-positive *Bacillus subtilis* and the least potent was against *Pseudomonas aeruginosa*. Compound **16** was selected to be conjugated with CuONPs and synthesize two nanoformulations. The 16-CuONPs synthesized by the aid of gamma irradiation (4.5 KG), exhibited moderate activity towards the selected strains. While the 16-CNPs displayed

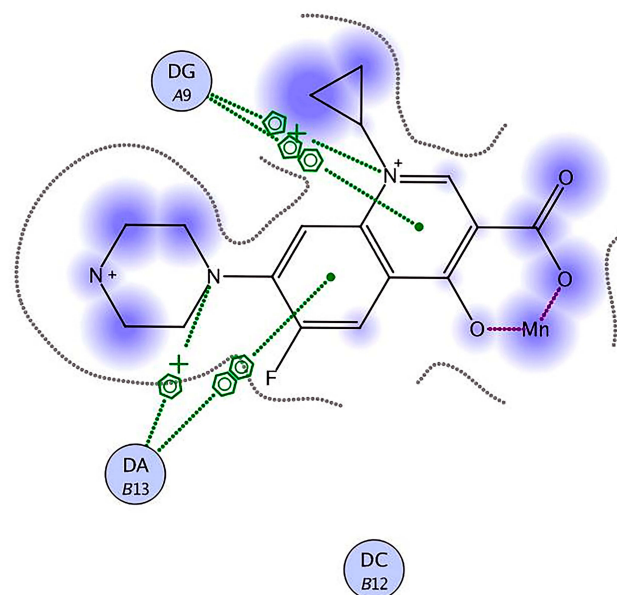


**Figure 12** Ciprofloxacin binds inside the active site of 2XCT to the DNA fragments DG:A9 & DA:B13 and Mn<sup>2+</sup>.

**Table 5** Determination of the Inhibitory Activity of Compound **16** and the Nanoformulations on *S. aureus* DNA Gyrase Enzyme

Code	<i>S. aureus</i> DNA Gyrase IC <sub>50</sub> (µg/mL)
Compound <b>16</b>	16.21 ± 1.10
CNPs	27.32 ± 1.56
16-CNPs	14.26 ± 0.68
16-CuONPs	12.49 ± 0.24
16-CuONPs-CNPs	10.57 ± 0.71
Ciprofloxacin	8.72 ± 0.64

**Table 6** Cytotoxicity of compound **16** and its nanoformulations on normal VERO cell Line

Compound No.	IC <sub>50</sub> (µg/mL)
16	927.28 ± 0.17
16-CNPs	543.37 ± 0.25
16- CuONPs-CNPs	637.69 ± 0.5

inhibition zones and MIC in the ranges of 29–43 mm and 0.07–2.50 µg/mL, and were more potent than CNPs. The nanocomposites 16-CuONPs-CNPs synthesized from compound **16** and CuONPs and encapsulated in chitosan proved to be the most potent nano formula and showed inhibition zones and MIC in the ranges of 34–45 mm and 0.03–1.25 µg/mL, respectively. Measurement of the MIC and MBC of the nanoformulations has confirmed their bactericidal and fungicidal activity. In vitro enzyme assay screening of compound **16** and the nanoformulations revealed that 16-CuONPs-CNPs showed the most potent inhibitory activity towards *S. aureus* DNA gyrase that is relatively equipotent to that of ciprofloxacin (IC<sub>50</sub>=10.57 versus 8.72 µg/mL, respectively). Cytotoxic activity

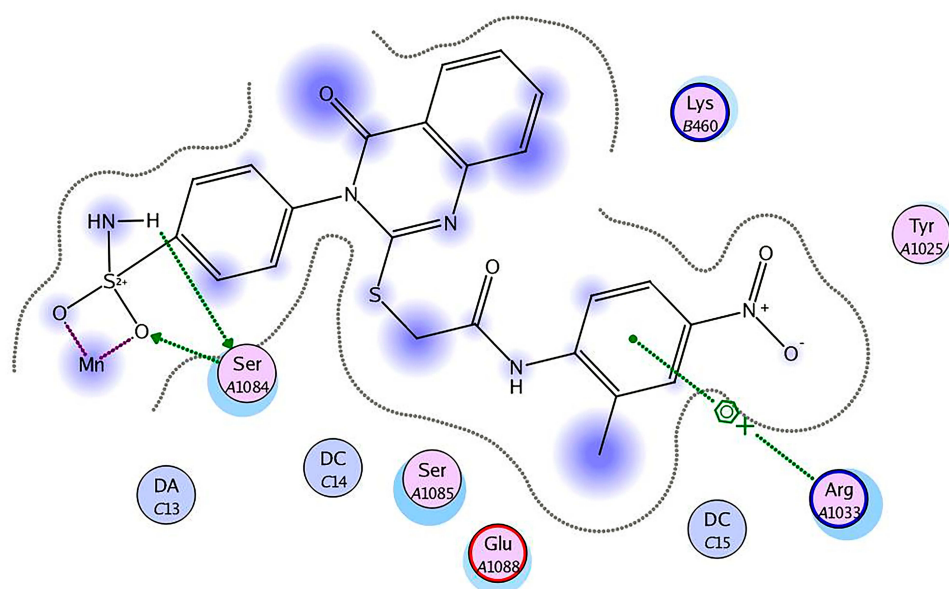


**Figure 13** Compound **16** forms hydrogen bonds with Ser A1084, cation- $\pi$  interaction with Arg A1033 and  $Mn^{2+}$ .

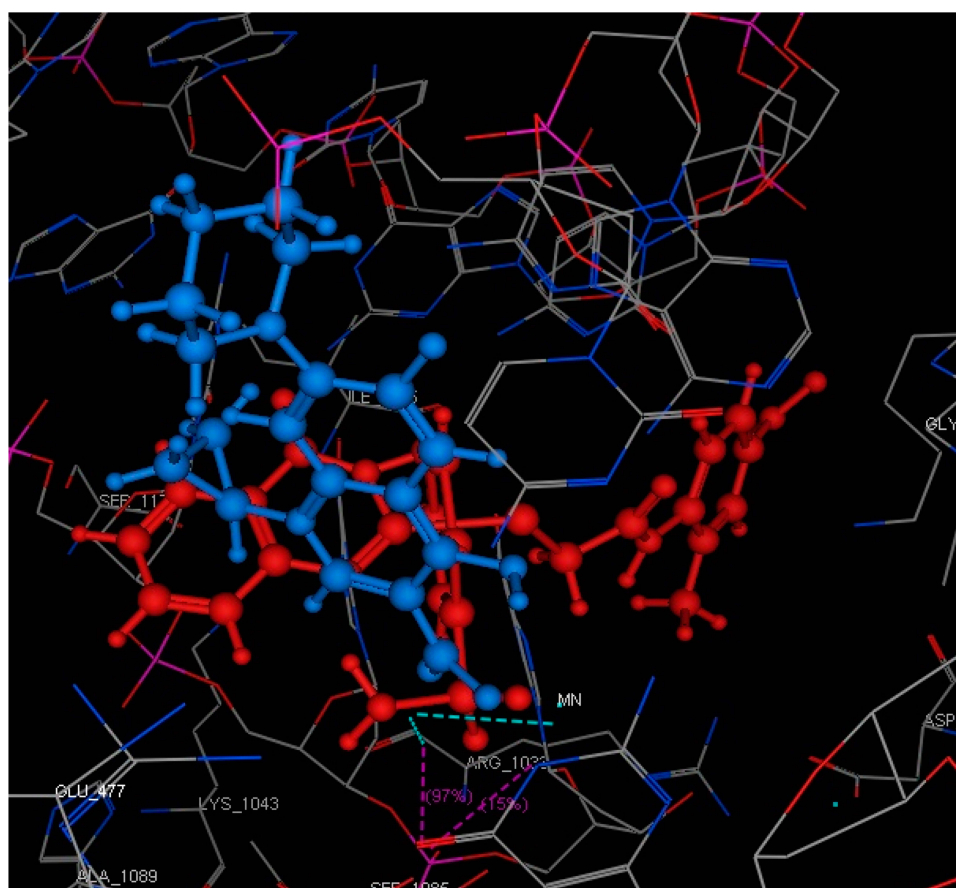


**Figure 14** Superimposition of compound **16** (red) and ciprofloxacin (blue) in which the  $SO_2$  group of **16** and the carboxylic of ciprofloxacin are directed towards the  $Mn^{2+}$ .

**Table 7** Docking Results of Compound **16** in the Active Site of *S. aureus* Gyrase Active Site (PDB: 2XCT)

Compound	Energy Score (S) (Kcal/mol)	Amino Acids	Interacting Groups	Length (Å)
<b>16</b>	−8.82	Ser 1084	SO <sub>2</sub>	2.28
		Ser 1084	NH <sub>2</sub>	2.52
		Arg 1033	Ph	4.07

screening of **16**, 16-CNPs and 16-CuONPs-CNPs on normal VERO cell line has proved their relative safety. Molecular docking of **16** revealed its proper binding inside the active site of *S. aureus* DNA gyrase, which may incorporate at least in part to its antimicrobial activity. Finally, hybridization between quinazolinone and benzenesulfonamide can provide potent antimicrobial candidates. The use of nanoformulations for the most potent compound has increased its potency against pathogenic microbes with multi-drug resistance such as MRSA. It is clear that compound **16** could be considered as a promising antimicrobial agent with enhanced activity upon nanoformulation.

## Acknowledgment

M.M. Ghorab and A.M. Soliman appreciate the staff members of the gamma irradiation unit at the National Center for Radiation Research and Technology (NCRRT) for carrying out the irradiation process.

A.S. Alqahtani is thankful to the Researchers Supporting Project number (RSP-2019/132), King Saud University, Riyadh, Saudi Arabia.

## Disclosure

The authors declare no conflict of interest.

## References

- Zhang L, Peng XM, Damu GL, Geng RX, Zhou CH. Comprehensive review in current developments of imidazole-based medicinal chemistry. *Med Res Rev*. 2014;34(2):340–437. doi:10.1002/med.21290.
- Peng X-M, Cai G-X, Zhou C-H. Recent developments in azole compounds as antibacterial and antifungal agents. *Curr Top Med Chem*. 2013;13(16):1963–2010. doi:10.2174/15680266113139990125
- Cui S-F, Addla D, Zhou C-H. Novel 3-aminothiazolquinolones: design, synthesis, bioactive evaluation, sars, and preliminary antibacterial mechanism. *J Med Chem*. 2016;59(10):4488–4510. doi:10.1021/acs.jmedchem.5b01678
- Zhang H-Z, Jeyakkumar P, Kumar KV, Zhou C-H. Synthesis of novel sulfonamide azoles via C–N cleavage of sulfonamides by azole ring and relational antimicrobial study. *New J Chem*. 2015;39(7):5776–5796. doi:10.1039/C4NJ01932F
- Jang M-Y, De Jonghe S, Segers K, Anné J, Herdewijn P. Synthesis of novel 5-amino-thiazolo [4, 5-d] pyrimidines as *E. coli* and *S. aureus* SecA inhibitors. *Bioorg Med Chem*. 2011;19(1):702–714. doi:10.1016/j.bmc.2010.10.027
- Khatkar A, Nanda A, Kumar P, Narasimhan B. Synthesis, antimicrobial evaluation and QSAR studies of p-coumaric acid derivatives. *Arab J Chem*. 2017;10:S3804–S3815. doi:10.1016/j.arabjc.2014.05.018
- Manikprabhu D, Lingappa K. Antibacterial activity of silver nanoparticles against methicillin-resistant *Staphylococcus aureus* synthesized using model *Streptomyces* sp. pigment by photo-irradiation method. *J Pharm Res*. 2013;6(2):255–260. doi:10.1016/j.jopr.2013.01.022
- Durán N, Marcato PD, De Souza GI, Alves OL, Esposito E. Antibacterial effect of silver nanoparticles produced by fungal process on textile fabrics and their effluent treatment. *J Biomed Nanotechnol*. 2007;3(2):203–208. doi:10.1166/jbn.2007.022
- Panagiotopoulos A, Zafropoulos TF, Perlepes SP, et al. Molecular structure and magnetic properties of acetato-bridged lanthanide (III) dimers. *Inorg Chem*. 1995;34(19):4918–4920. doi:10.1021/ic00123a029
- El-Nawawy M, Farag R, Sabbah I, Abu-Yamin A. Synthesis, spectroscopic, thermal studies and biological activity of a new sulfamethoxazole schiff base and its copper complexes. *Int J Pharm Sci Res*. 2011;2(12):3143–3148.
- Chevalier J, Mahamoud A, Baitiche M, et al. Quinazoline derivatives are efficient chemosensitizers of antibiotic activity in *Enterobacter aerogenes*, *Klebsiella pneumoniae* and *Pseudomonas aeruginosa* resistant strains. *Int J Antimicrob Agents*. 2010;36(2):164–168. doi:10.1016/j.ijantimicag.2010.03.027
- Ghorab M, AbdelHamide S, ElHakim A. Synthesis of some new biologically active 2-phenyl-6-iodo-3-substituted-4 (3H) quinazolinones. *Indian J Heterocycl Chem*. 1995;5(2):115–120.
- Mahamoud A, Chevalier J, Baitiche M, Adam E, Pages J-M. An alkylaminoquinazoline restores antibiotic activity in Gram-negative resistant isolates. *Microbiology*. 2011;157(2):566–571. doi:10.1099/mic.0.045716-0
- Devi KA, Sarangapani M. Synthesis and antimicrobial activity of some quinazolinones derivatives. *Int J Drug Dev Res*. 2012;4(3):324–327.
- Jafari E, Khajouei MR, Hassanzadeh F, Hakimelahi GH, Khodarahmi GA. Quinazolinone and quinazoline derivatives: recent structures with potent antimicrobial and cytotoxic activities. *Res Pharm Sci*. 2016;11(1):1–14.
- Suresha G, Suhas R, Kapfo W, Gowda DC. Urea/thiourea derivatives of quinazolinone–lysine conjugates: synthesis and structure–activity relationships of a new series of antimicrobials. *Eur J Med Chem*. 2011;46(6):2530–2540. doi:10.1016/j.ejmech.2011.03.041
- Al-Omary FA, Hassan GS, El-Messery SM, Nagi MN, Habib E-SE, El-Subbagh HI. Nonclassical antifolates, part 3: synthesis, biological evaluation and molecular modeling study of some new 2-heteroarylthioquinazolin-4-ones. *Eur J Med Chem*. 2013;63:33–45. doi:10.1016/j.ejmech.2012.12.061
- Dinakaram M, Selvam P, DeClercq E, Sridhar SK. Synthesis, antiviral and cytotoxic activity of 6-bromo-2, 3-disubstituted-4 (3H)-quinazolinones. *Biol Pharm Bull*. 2003;26(9):1278–1282. doi:10.1248/bpb.26.1278
- Lubenets V, Karpenko O, Ponomarenko M, Zahoriy G, Krychkovska A, Novikov V. *Development of New Antimicrobial Compositions of Thiosulfonate Structure*. 2013:119–124.
- Lubenets V, Vasylyuk S, Monka N, et al. Synthesis and antimicrobial properties of 4-acylaminobenzenethiosulfoacid S-esters. *Saudi Pharm J*. 2017;25(2):266–274. doi:10.1016/j.jsps.2016.06.007
- Elgadir MA, Uddin MS, Ferdosh S, Adam A, Chowdhury AJK, Sarker MZI. Impact of chitosan composites and chitosan nanoparticle composites on various drug delivery systems: a review. *J Food Drug Anal*. 2015;23(4):619–629. doi:10.1016/j.jfda.2014.10.008



22. Park JH, Saravanakumar G, Kim K, Kwon IC. Targeted delivery of low molecular drugs using chitosan and its derivatives. *Adv Drug Deliv Rev.* 2010;62(1):28–41. doi:10.1016/j.addr.2009.10.003
23. Wu T, Wu C, Fu S, et al. Integration of lysozyme into chitosan nanoparticles for improving antibacterial activity. *Carbohydr Polym.* 2017;155:192–200. doi:10.1016/j.carbpol.2016.08.076
24. Mendoza G, Regiel-Futyr A, Andreu V, et al. Bactericidal effect of gold–chitosan nanocomposites in coculture models of pathogenic bacteria and human macrophages. *ACS Appl Mater Interfaces.* 2017;9(21):17693–17701. doi:10.1021/acsami.6b15123
25. Usman MS, El Zowalaty ME, Shameli K, Zainuddin N, Salama M, Ibrahim NA. Synthesis, characterization, and antimicrobial properties of copper nanoparticles. *Int J Nanomedicine.* 2013;8:4467–4479. doi:10.2147/IJN.S50837
26. Salehi E, Daraei P, Shamsabadi AA. A review on chitosan-based adsorptive membranes. *Carbohydr Polym.* 2016;152:419–432. doi:10.1016/j.carbpol.2016.07.033
27. Ramyadevi J, Jeyasubramanian K, Marikani A, Rajakumar G, Rahuman AA. Synthesis and antimicrobial activity of copper nanoparticles. *Mater Lett.* 2012;71:114–116. doi:10.1016/j.matlet.2011.12.055
28. Khashan KS, Sulaiman GM, Abdulameer FA. Synthesis and antibacterial activity of CuO nanoparticles suspension induced by laser ablation in liquid. *Arab J Sci Eng.* 2016;41(1):301–310. doi:10.1007/s13369-015-1733-7
29. Emami-Karvani Z, Chehrizi P. Antibacterial activity of ZnO nanoparticle on gram-positive and gram-negative bacteria. *Afr J Microbiol Res.* 2011;5(12):1368–1373.
30. Gong -H-H, Addla D, Lv J-S, Zhou C-H. Heterocyclic naphthalimides as new skeleton structure of compounds with increasingly expanding relational medicinal applications. *Curr Top Med Chem.* 2016;16(28):3303–3364. doi:10.2174/1568026616666160506145943
31. Ghorab MM, Alsaid MS, Soliman AM, Al-Mishari AA. Benzo [g] quinazolin-based scaffold derivatives as dual EGFR/HER2 inhibitors. *J Enzyme Inhib Med Chem.* 2018;33(1):67–73. doi:10.1080/14756366.2017.1389922
32. Ghorab MM, Alsaid MS, Soliman AM, Ragab FA. VEGFR-2 inhibitors and apoptosis inducers: synthesis and molecular design of new benzo [g] quinazolin bearing benzenesulfonamide moiety. *J Enzyme Inhib Med Chem.* 2017;32(1):893–907. doi:10.1080/14756366.2017.1334650
33. Alsaid MS, Al-Mishari AA, Soliman AM, Ragab FA, Ghorab MM. Discovery of Benzo [g] quinazolin benzenesulfonamide derivatives as dual EGFR/HER2 inhibitors. *Eur J Med Chem.* 2017;141:84–91. doi:10.1016/j.ejmech.2017.09.061
34. Ghorab MM, Alsaid MS, El-Gaby MS, Safwat NA, Elaasser MM, Soliman AM. Biological evaluation of some new N-(2, 6-dimethoxypyrimidinyl) thioureido benzenesulfonamide derivatives as potential antimicrobial and anticancer agents. *Eur J Med Chem.* 2016;124:299–310. doi:10.1016/j.ejmech.2016.08.060
35. Ghorab MM, Soliman AM, Alsaid MS, Askar AA. Synthesis, antimicrobial activity and docking study of some novel 4-(4, 4-dimethyl-2, 6-dioxocyclohexylidene) methylamino derivatives carrying biologically active sulfonamide moiety. *Arab J Chem.* 2020;13(1):545–556. doi:10.1016/j.arabjc.2017.05.022
36. Murugavel S, Sundramoorthy S, Lakshmanan D, Subashini R, Kumar PP. Synthesis, crystal structure analysis, spectral (NMR, FT-IR, FT-Raman and UV–Vis) investigations, molecular docking studies, antimicrobial studies and quantum chemical calculations of a novel 4-chloro-8-methoxyquinoline-2 (1H)-one: an effective antimicrobial agent and an inhibition of DNA gyrase and lanosterol-14 $\alpha$ -demethylase enzymes. *J Mol Struct.* 2017;1131:51–72. doi:10.1016/j.molstruc.2016.11.035
37. Leshner GY, Froelich EJ, Gruett MD, Bailey JH, Brundage RP. 1, 8-Naphthyridine derivatives. A new class of chemotherapeutic agents. *J Med Chem.* 1962;5(5):1063–1065. doi:10.1021/jm01240a021
38. Soliman AM, Ghorab MM. Exploration of N-alkyl-2-[(4-oxo-3-(4-sulfamoylphenyl)-3, 4-dihydroquinazolin-2-yl) thio] acetamide derivatives as anticancer and radiosensitizing agents. *Bioorg Chem.* 2019;88:102956. doi:10.1016/j.bioorg.2019.102956
39. Cappuccino J, Sherman N. *Microbiology, Laboratory Manual.* India: Pearson Education, Inc New Delhi; 2004:282–283.
40. Cooper K. The theory of antibiotic inhibition zones. *Anal Microbiol.* 1963;1–86.
41. Hassan AS, Askar AA, Nossier ES, Naglah AM, Moustafa GO, Al-Omar MA. Antibacterial evaluation, in silico characters and molecular docking of schiff bases derived from 5-aminopyrazoles. *Molecules.* 2019;24(17):3130. doi:10.3390/molecules24173130
42. Wikler M, Hindler J, Cockerill F, et al. *Methods for Dilution Antimicrobial Susceptibility Tests for Bacteria That Grow Aerobically; Approved Standard; CLSI Document M07-A8; ISBN: ISBN 1-56238-689-1.* Wayne, PA, USA: Clinical and Laboratory Standards Institute; 2008.
43. Kawashima Y, Handa T, Kasai A, Takenaka H, Lin S, Ando Y. Novel method for the preparation of controlled-release theophylline granules coated with a polyelectrolyte complex of sodium polyphosphate–chitosan. *J Pharm Sci.* 1985;74(3):264–268. doi:10.1002/jps.2600740308
44. Dias FR, Novais JS, Devillart T, et al. Synthesis and antimicrobial evaluation of amino sugar-based naphthoquinones and isoquinoline-5, 8-diones and their halogenated compounds. *Eur J Med Chem.* 2018;156:1–12. doi:10.1016/j.ejmech.2018.06.050
45. Alt S, Mitchenall LA, Maxwell A, Heide L. Inhibition of DNA gyrase and DNA topoisomerase IV of *Staphylococcus aureus* and *Escherichia coli* by aminocoumarin antibiotics. *J Antimicrob Chemother.* 2011;66(9):2061–2069. doi:10.1093/jac/ckr247
46. Ghorab MM, El Ella DAA, Heiba HI, Soliman AM. Synthesis of certain new thiazole derivatives bearing a sulfonamide moiety with expected anticancer and radiosensitizing activities. *J Mater Sci Eng A.* 2011;1:684–691.
47. Berne BJ, Pecora R. *Dynamic Light Scattering: With Applications to Chemistry, Biology, and Physics.* Courier Corporation; 2000.
48. El-Batal A, El-Sayed MH, Refaat BM, Askar AAZ. Marine streptomyces cyaneus strain alex-SK121 mediated eco-friendly synthesis of silver nanoparticles using gamma radiation. *Br J Pharm Res.* 2014;4(21):2525–2547. doi:10.9734/BJPR/2014/12224
49. Etefagh R, Azhir E, Shahtahmasebi N. Synthesis of CuO nanoparticles and fabrication of nanostructural layer biosensors for detecting *Aspergillus niger* fungi. *Sci Iran.* 2013;20(3):1055–1058.
50. Clark J. *Joint Committee on Powder Diffraction Standards (JCPDS).* 1961. In Card.
51. Sun N, Li M, Cai S, et al. Antibacterial evaluation and mode of action study of BIMQ, a novel bacterial cell division inhibitor. *Biochem Biophys Res Commun.* 2019;514(4):1224–1230. doi:10.1016/j.bbrc.2019.05.086
52. Keepers YP, Pizao PE, Peters GJ, van Ark-otte J, Winograd B, Pinedo HM. Comparison of the sulforhodamine B protein and tetrazolium (MTT) assays for in vitro chemosensitivity testing. *Eur J Cancer Clin Oncol.* 1991;27(7):897–900. doi:10.1016/0277-5379(91)90142-Z
53. Bax BD, Chan PF, Eggleston DS, et al. Type IIA topoisomerase inhibition by a new class of antibacterial agents. *Nature.* 2010;466(7309):935. doi:10.1038/nature09197



**International Journal of Nanomedicine****Dovepress****Publish your work in this journal**

The International Journal of Nanomedicine is an international, peer-reviewed journal focusing on the application of nanotechnology in diagnostics, therapeutics, and drug delivery systems throughout the biomedical field. This journal is indexed on PubMed Central, MedLine, CAS, SciSearch<sup>®</sup>, Current Contents<sup>®</sup>/Clinical Medicine,

Journal Citation Reports/Science Edition, EMBase, Scopus and the Elsevier Bibliographic databases. The manuscript management system is completely online and includes a very quick and fair peer-review system, which is all easy to use. Visit <http://www.dovepress.com/testimonials.php> to read real quotes from published authors.

Submit your manuscript here: <https://www.dovepress.com/international-journal-of-nanomedicine-journal>